THE JOURNAL OF BIOLOGICAL CHEMISTRY
Vol. 277, No. 46, Issue of November 15, pp. 44417–44430, 2002
Printed in U.S.A.

Phosphorylation of p85 βPIX, a Rac/Cdc42-specific Guanine Nucleotide Exchange Factor, via the Ras/ERK/PAK2 Pathway Is Required for Basic Fibroblast Growth Factor-induced Neurite Outgrowth*

Received for publication, April 18, 2002, and in revised form, August 20, 2002
Published, JBC Papers in Press, September 10, 2002, DOI 10.1074/jbc.M203754200

Eun-Young Shin‡§, Kyung-Sun Shin§¶, Chan-Soo Lee‡, Kyung-Nam Woo‡, Song-Hua Quan‡, Nak-Kyun Soung‡, Young Gyu Kim‖, Choong Ik Cha, Seung-Ryul Kim‡, Dongeun Park‡‡, Gary M. Bokoch§§, and Eung-Gook Kim‡¶¶**

*From the Department of ‡Biochemistry and ‖Neurosurgery, College of Medicine, Chungbuk National University, Cheongju 361-763, ¶Biotechnology Research Team, R & D Center, Daewoong Pharmaceutical Company, Yongin 449-814, the **Department of Anatomy, Seoul National University College of Medicine, Seoul 110-799, ‡‡School of Biological Sciences, Seoul National University, Seoul 151-742, Korea, and the §§Departments of Immunology and Cell Biology, The Scripps Research Institute, La Jolla, California 92037*

Guanine nucleotide exchange factors (GEFs) have been implicated in growth factor-induced neuronal differentiation through the activation of small GTPases. Although phosphorylation of these GEFs is considered an activation mechanism, little is known about the upstream of PAK-interacting exchange factor (PIX), a member of the Dbl family of GEFs. We report here that phosphorylation of p85 βPIX/Cool/p85SPR is mediated via the Ras/ERK/PAK2 pathway. To understand the role of p85 βPIX in basic fibroblast growth factor (bFGF)-induced neurite outgrowth, we established PC12 cell lines that overexpress the fibroblast growth factor receptor-1 in a tetracycline-inducible manner. Treatment with bFGF induces the phosphorylation of p85 βPIX, as determined by metabolic labeling and mobility shift upon gel electrophoresis. Interestingly, phosphorylation of p85 βPIX is inhibited by PD98059, a specific MEK inhibitor, suggesting the involvement of the ERK cascade. PAK2, a major PAK isoform in PC12 cells as well as a binding partner of p85 βPIX, also functions upstream of p85 βPIX phosphorylation. Surprisingly, PAK2 directly binds to ERK, and its activation is dependent on ERK. p85 βPIX specifically localizes to the lamellipodia at neuronal growth cones in response to bFGF. A mutant form of p85 βPIX (S525A/T526A), in which the major phosphorylation sites are replaced by alanine, shows significant defect in targeting. Moreover, expression of the mutant p85 βPIX efficiently blocks PC12 cell neurite outgrowth. Our study defines a novel signaling pathway for bFGF-induced neurite outgrowth that involves activation of the PAK2-p85 βPIX complex via the ERK cascade and subsequent translocation of this complex.

The activities of small GTP-binding proteins (G proteins) are tightly regulated by guanine nucleotide exchange factors (GEFs),[1] GTPase-activating proteins, and guanine nucleotide dissociation inhibitors. GEFs stimulate activation of small G proteins by catalyzing GDP/GTP exchange. GEFs of the Dbl family function immediately upstream of Rho family G proteins (1), which play a critical role in cytoskeletal reorganization (2). Recent evidence suggests a role for Rho family G proteins during developmental neuritogenesis (3–5) and in the regeneration of the nervous system (6, 7). Rac1 and Cdc42 likely promote neurite outgrowth through the formation of lamellipodia and filopodia at growth cones, respectively (8–12). In contrast, RhoA mediates growth cone collapse and neurite retraction with concomitant cell rounding (13–15). Dominant negative constructs of Rac1 or Cdc42 eliminate neurite extension induced by nerve growth factor (NGF) (16, 17), suggesting that NGF can initiate intracellular signals that are conveyed to these Rho GTPases and to their upstream GEFs (18–20). Growth factors such as NGF and basic fibroblast growth factor (bFGF) are potent extracellular stimuli for neurite outgrowth in PC12 cells, a model system that has been widely used to understand the molecular mechanism of neurite outgrowth. Therefore, it seems reasonable to assume that bFGF also activates the specific GEFs for Rac1 and Cdc42. However, the signaling pathway that links bFGF to these GEFs has not yet been delineated.

The p21-activated kinase (PAK) is central to cytoskeletal changes associated with neurite outgrowth in PC12 cells (21). The PAK family constitutes six distinct members, PAK1–6 (22), and their activities are up-regulated by interaction with the GTP-bound forms of active Rac1 or Cdc42 via a specific p21-binding domain in the N terminus (23, 24). Thus, PAK has been thought to be a downstream effector of Rac1 and Cdc42. It

* This work was supported in part by Grant RO1-2000-000-00112-0 from the Korean Science and Engineering Foundation, Grant PJ1-PG3-21300-0007 from the Korea Health and Welfare, Republic of Korea, Grant GM39434 from the National Institutes of Health (to G. M. B.), and a grant from the Ministry of Science and Technology through the Brain Science Research Program (to D. P.). The costs of publication of this article were defrayed in part by the payment of page charges. This article must therefore be hereby marked "*advertisement*" in accordance with 18 U.S.C. Section 1734 solely to indicate this fact.

§ Both authors contributed equally to this work.

¶¶ To whom correspondence should be addressed: Dept. of Biochemistry, College of Medicine, Medical Research Institute, and Biotechnology Research Institute, Chungbuk National University, San 48, Gaesin-dong, Heungduk-ku, Cheongju, Korea, 361-763. Tel.: 82-43-261-2848; Fax: 82-43-274-9710; E-mail: egkim@med.chungbuk.ac.kr.

[1] The abbreviations used are: GEFs, guanine nucleotide exchange factors; PIX, PAK-interacting exchange factor; bFGF, basic fibroblast growth factor; FGF, fibroblast growth factor; PAK, p21-activated kinase; ERK, extracellular signal-regulated protein kinase; MAPK, mitogen-activated protein kinase; MEK, MAPK/ERK kinase; DN, dominant negative; GFP, green fluorescent protein; EGFP, enhanced GFP; NGF, nerve growth factor; DMEM, Dulbecco's modified Eagle's medium; FBS, fetal bovine serum; PBS, phosphate-buffered saline; FGFR-1, FGF receptor-1; PVDF, polyvinylidene difluoride; MBP, myelin basic protein; SH, Src homology; DH, Dbl homology; PH, pleckstrin homology; GB, GIT1-binding; PI3-kinase, phosphatidylinositol 3-kinase; PID, PAK inhibitory domain; GST, glutathione *S*-transferase; bFGF, basic FGF.

is somewhat surprising that Rac1/Cdc42-binding deficient PAK1 mutants induce a Rac phenotype in PC12 cells, because this result suggests that PAK acts upstream of Rac1 under certain circumstances and that its p21-binding domain is dispensable (25). Consistent with this, expression of the membrane targeting form of kinase-negative PAK1 also causes morphological changes similar to those observed with wild type PAK1 (26). It has been demonstrated further that the membrane targeting of PAK1 is sufficient for neurite outgrowth in PC12 cells, suggesting that the major downstream mediators of PAK for cytoskeletal remodeling reside in the membrane. Given that PAK functions upstream of Rac1 and that targeting of PAK to the membrane is sufficient for neurite outgrowth, elucidation of the mechanism by which PAK is targeted to the membrane seems to be a prerequisite to understand how PAK exerts its effect on the actin cytoskeleton.

Nck is an adaptor protein containing a single Src homology 2 (SH2) domain and three SH3 domains (27). Nck is constitutively associated with PAK1, and association is mediated through the interaction between the second SH3 domain of Nck and the first proline-rich sequence of PAK (28–31). On the other hand, the SH2 domain of Nck binds with high affinity to tyrosine-phosphorylated receptor kinases such as the platelet-derived growth factor receptor and the epidermal growth factor receptor (32–35). Therefore, the Nck-PAK complex might be relocalized to the membrane by recruitment to the receptor tyrosine kinases upon growth factor stimulation (29, 36). Membrane-targeted PAK has been shown to possess an enhanced kinase activity and to activate downstream mitogen-activated protein kinases (MAPKs), including ERK1 (30). However, overexpression of Nck inhibits both the NGF- and bFGF-induced neurite outgrowth in PC12 cells, suggesting that proteins other than PAK are major downstream effectors and are more potent in inducing the proliferation of PC12 cells (37). Nck-mediated PAK translocation and activation provide a clue that SH3 adaptor molecules other than PAK might be involved in the translocation of PAK.

Recently, the PIX (PAK-interacting exchange factor)/Cool (cloned out of library) protein has been identified as a new PAK-binding partner (21). PIX was first cloned as p85SPR (SH3 domain-containing proline-rich protein) (38). The PIX family contains two members, αPIX and βPIX. βPIX exists as two distinct isoforms, β1 and β2, that are distinguished by the presence of a C-terminal coiled-coil leucine zipper domain (39). The primary β1PIX transcript can be spliced to produce three variants, β1PIX-a, β1PIX-b, and β1PIX-c (40). Adding to the complexity, β1PIX-a (identical to p85SPR/p85Cool-1, which we designate p85 βPIX) can be expressed as a shorter protein, p50Cool (41, 42). All these isoforms share SH3, Dbl homology (DH), and pleckstrin homology (PH) domains at their N termini. The SH3 domain of PIX binds to a unique proline-rich PAK sequence (P*XXX*P) located between the third and the fourth conventional SH3-binding motif (P*XX*P). Through this interaction the PIX-PAK complex gains the much higher affinity (K_d of 24 nM) than the Nck-PAK complex and co-localizes in focal complex (21). Other domains of PIX, a GIT1-binding (GB) domain and a leucine zipper domain, are tandemly arranged at the C terminus. The GB domain is a site for interaction with ADP-ribosylation factor-GTPase-activating proteins such as Cat (cool-associated, tyrosine-phosphorylated), p95PKL (paxillin-kinase linker), and GIT (G-protein-coupled receptor kinase-interacting targets) (43–45). The leucine zipper domain at the C terminus was recently shown to mediate the homodimerization of PIX, which is essential for several features of cytoskeletal reorganization, such as membrane ruffles (46). αPIX has an additional calponin homology domain at the N terminus compared with βPIX.

PIX exhibits a GEF activity toward both Rac1 and Cdc42 *in vitro* and *in vivo* (21). αPIX is activated by interaction with phosphatidylinositol 3-kinase (PI3-kinase) in the signaling pathway from the platelet-derived growth factor receptor and from the EphB2 receptor as well as in the integrin-induced signaling (47). As a result of this signaling, αPIX is redistributed to the membrane by forming a complex with these receptors via direct association with the p85 regulatory subunit of PI3-kinase, and its GEF activity is enhanced by the membrane-targeted PI3-kinase. However, little is known about the signaling pathway of βPIX activation. In the present study, we show that p85 βPIX is phosphorylated in response to bFGF, and its upstream pathway is defined by the components Ras/Raf-1/MEK/ERK/PAK2. p85 βPIX has been shown to be constitutively associated with PAK2, a major PAK isoform in PC12 cells. Basic FGF induces phosphorylation of p85 βPIX through activation of PAK2, which acts downstream of the Ras/ERK cascade. Translocation of p85 βPIX to the lamellipodia at growth cones is dependent on this phosphorylation. These results suggest that the PAK2-dependent phosphorylation of p85 βPIX is a signal for targeting of the p85 βPIX-PAK2 complex to the lamellipodia at growth cones, where PAK2 regulates reorganization of the actin cytoskeleton for bFGF-induced neurite extension in PC12 cells.

EXPERIMENTAL PROCEDURES

Materials—[^{32}P]H_3PO_4 (3,000 Ci/mmol), [γ-^{32}P]ATP, and ^{125}I-labeled bFGF were purchased from PerkinElmer Life Sciences. Staurosporine, calphostin C, LY294002, KN-62, K-252a, genistein, and PD98059 were purchased from Calbiochem. Alkaline phosphatase and protein phosphatase 2A were purchased from Roche Molecular Biotechnology and Upstate Biotechnology, Inc. (Lake Placid, NY), respectively. Human recombinant bFGF, LipofectAMINE 2000, G418, and hygromycin B were obtained from Invitrogen. Mouse monoclonal antibodies to ERK (total ERK1/2, and phospho-specific ERK1/2) were purchased from New England Biolabs (Beverly, MA). The glutathione-Sepharose-bound GST-ERK1 protein was purchased from Upstate Biotechnology, Inc. (Lake Placid, NY). Anti-PAK antibodies were purchased from Santa Cruz Biotechnology (Santa Cruz, CA). Anti-p85 βPIX antibody was raised against the SH3 domain of p85 βPIX (46). The QuikChange Site-directed mutagenesis kit was purchased from Stratagene (La Jolla, CA). The Tet-on system, pEGFP-C2, pDS-RED2-C1, and anti-GFP antibody were purchased from Clontech (Palo Alto, CA). PC12DN-Ras is a gift from Dr. H. Y. Yoon (College of Medicine, Chung-Ang University, Seoul, Korea). This cell line is a stable transfectant of pTRE-DN-Ras encoding a dominant negative form of Ras (N17 Ras), which is expressed in a doxycycline-inducible manner.

Plasmids and DNA Constructs—FGF receptor-1 (FGFR-1) cDNA for inducible expression was amplified by the PCR from rat FGFR-1 cDNA (48) and cloned into *Eco*RI/*Xba*I sites of pTRE (Clontech). Primers were used as follows: 5′ primer (5′-GAATCCATGTGGGGCTGGAGGGGC-CTC-3′) and 3′ primer (5′-TCTAGATCAGCGCCGGTTGAGTCCG-3′). The p85 βPIX construct was amplified using mouse p85 βPIX cDNA (identical to β1PIX-a isoform) as template (38), followed by introduction into the *Xho*I/*Eco*RI sites of pEGFP-C2 or pDS-Red2-C1 (Clontech). PAK2 cDNA was retrieved by reverse transcriptase-PCR from PC12 cell mRNAs, using the following primers: 5′ primer (5′-AGATCTATGTCT-GATAACGGGAGCTA-3′) and 3′ primer (5′-GAATTCTTAGCGGT-TACTCTTCATTGC-3′) and subcloned into *Bgl*II/*Eco*RI sites of pEGFP-C2. To express in *Escherichia coli* PAK1 and PAK2, cDNAs were subcloned into a pQE vector. Primers for PCR cloning were as follows: 5′ primer (5′-GCATGCAAATGTCAAATAACGGCCTAGAC-3′) and 3′ primer (5′-AGATCTTCTCACAGAGCTTGGCAC-3′) for PAK1, and 5′ primer (5′-CCATGGCTATGTCTGATAACGGGGAGCTA-3′) and 3′ primer (5′-AGATCTGCGGTTACTCTTCATTGCTTC-3′) for PAK2. The PAK2 deletion construct (residues 1–327) was generated from amplification using the following primers, followed by subcloning into *Bgl*II site of pEGFP: 5′ primer (5′-AGATCTATGTCTGATTAACGGGGAGCT-3′) and 3′ primer (5′-AGATCTAGCAAGGTACTCCATTAC-3′). To generate mutant cDNAs, mutagenesis was conducted using the QuikChange site-directed mutagenesis kit (Stratagene) according to the manufactur-

er's recommendation. The p85 βPIX mutant (S525A/T526A) was generated by mutagenic PCR using sense (5′-GCTGTGCGCAAGGCCGCAGCGGCGCTGGAAGC-3′) and antisense (5′-TTCCAGCGCCGCTGCGGCCTTGCGCACAGC-3′) oligonucleotides. The PAK1 (T423E), PAK2 (T402E), and PAK2 (P185A/R186A) mutants were generated by mutagenic PCR using sense (5′-CAGAGCAAACGGAGCGAGATGGTAGGAACCCCA-3′, 5′-AGCAAACGCAGTGAGATGGTTGGAACGCCA-3′, and 5′-CCCGTCATTGCCGCTGCGCCAGATCATACA-3′) and antisense (5′-TGGGGTTCCTACCATCTCGCTCCGTTTGCTCGT-3′, 5′-TGGCGTTCCAACCATCTCACTGCGTTTGCT-3′, and 5′-TGTATGATCTGGCGCAGCGGCAATGACGGG-3′) primers, respectively. PAK inhibitory domain (PID) cDNA (226–447 bp) was amplified from human PAK1 with PID5 (5′-GAATTCCACACAATTCATGTCGG-3′) and PID3 (5′-GTCGACTAGATGACTTATCTGTAAAG C-3′) primers and subcloned into *Eco*RI/*Sal*I sites of pEGFP-C2. pTM-MEK-S218A/S222A (dominant negative MEK1) was kindly provided by Dr. K. C. Chung (College of Medicine, Yonsei University, Seoul, Korea).

Metabolic Labeling—PC12FW cells were incubated in phosphate-free DMEM containing doxycycline (1.5 μg/ml) for 24 h and stimulated for 4 h in the presence or absence of bFGF (10 ng/ml). During the stimulation, cells were labeled with [^{32}P]H_3PO_4 (0.3 mCi/ml). After aspiration of medium, cells were washed extensively with ice-cold phosphate-buffered saline (PBS; 150 mM NaCl, 10 mM Na_2HPO_4, 2.5 mM KCl, 1.5 mM KH_2PO_4) and lysed in lysis buffer (50 mM HEPES, pH 7.5, 150 mM NaCl, 100 mM NaF, 10% glycerol, 1% Triton X-100, 200 μM orthovanadate, 1 mM phenylmethylsulfonyl fluoride, 1 μg/ml aprotinin, 1 μg/ml leupeptin). The lysates were clarified by centrifugation for 20 min at 12,000 rpm and immunoprecipitated with anti-p85 βPIX antibody. Immunoprecipitates were washed five times with lysis buffer and twice with ice-cold PBS. Each sample was resuspended in SDS-PAGE sample buffer, boiled at 100 °C for 5 min, resolved by 8% SDS-PAGE, and transferred to a membrane. p85 βPIX was detected by autoradiography and confirmed by immunoblotting with anti-p85 βPIX antibody. For labeling of pEGFP-p85 βPIX, (wild type) or pEGFP-Mp85 βPIX (mutant type, S525A/T526A),transfected cells, the same procedure was employed except for immunoprecipitation with anti-GFP antibody.

Cell Culture and Differentiation—PC12-tet-on cells (Clontech) were routinely cultured on poly-L-lysine-coated tissue culture dishes in DMEM supplemented with 10% Tet System-approved fetal bovine serum (FBS) (Clontech), 2 mM glutamine, 1× antibiotics (Invitrogen), and 100 μg/ml G418. PC12FW cells were grown in the same medium supplemented with 50 μg/ml hygromycin B. Prior to differentiation, PC12FW cells were incubated in serum-free DMEM with 1.5 μg/ml doxycycline for 24 h to induce FGFR expression. Culture medium was then replaced by DMEM supplemented with 2% FBS, 10 ng/ml bFGF (Invitrogen), and 1.5 μg/ml doxycycline. bFGF-containing medium was changed every 48 h. After 2–4 days of bFGF treatment, cells showing a typical phenotype were captured by the SPOT system with an inverted phase contrast microscope (Fig. 1*B*). Transfected cells expressing green fluorescent protein (GFP) were monitored by fluorescence with a fluorescence microscope (Olympus, CK-40). bFGF-induced differentiation was measured by scoring as positive those green cells with one or more growth cone-tipped neurites longer than two cell bodies in length (26). Cells from at least 10 different microscope fields of view were counted with a fluorescence microscope.

Stable Transfection (Establishment of PC12FW Cell Lines)—Transfection was performed with the calcium phosphate transfection reagent (Invitrogen). Briefly, 1 μg of pTK-HYG and 10 μg of pTRE-FGFR-1 were resuspended in 0.3 ml of 2× HBS (0.5% HEPES, 0.8% NaCl, 0.1% dextrose, 0.01% anhydrous Na_2HPO_4, 0.37% KCl; pH adjusted to 7.05) and mixed with 36 μl of 2 M $CaCl_2$. The mixture was incubated at room temperature for 20 min prior to addition to the cells. Cells were grown for 24 h in nonselective culture medium and then replaced by complete DMEM containing 250 μg/ml hygromycin B (Invitrogen). After 14 days of culture in the hygromycin B-containing medium, hygromycin B-resistant colonies were isolated and transferred to 96-well plates. The selected colonies were subcloned to obtain populations of single cells, and selection pressure was maintained subsequently in the presence of 50 μg/ml hygromycin B and 100 μg/ml G418. To measure expression levels of FGFR-1, a receptor binding assay was conducted. Cells were incubated with 0.2 ng/ml ^{125}I-labeled bFGF in binding buffer (DMEM, 0.1% bovine serum albumin, 25 mM HEPES, pH 7.5) for 3 h at 4 °C and washed twice with a solution of 1.6 M NaCl in PBS, pH 7.5. To release ^{125}I-labeled bFGF from FGFR-1, cells were incubated in a solution of 2 M NaCl in PBS, pH 4.0, for 5 min. Expression levels of FGFR-1 were calculated by counting radioactivity of released ^{125}I-labeled bFGF. Nonspecific binding was determined in the presence of unlabeled recombinant bFGF.

Transient Transfection—PC12FW cells were seeded on sterilized glass coverslips that had been pre-coated with 20 μg/ml poly-L-lysine (Sigma) and inserted into 6-well plates (1×10^5 cells/well). For transfection and localization of proteins, PC12FW cells were induced to differentiate in complete media containing 10 ng/ml bFGF for 48 h and transfected with pEGFP-p85 βPIX or various vector constructs using LipofectAMINE 2000 (Invitrogen) according to the manufacturer's instructions. Transfected cells were incubated in DMEM containing 2% FBS in the presence or absence of 10 ng/ml bFGF for 24–48 h. Cells were washed three times with PBS and fixed in 4% paraformaldehyde/PBS for 15 min. After fixation the coverslips were washed twice in PBS and mounted onto a glass slide with gelvatol. Fluorescence was visualized with a laser confocal microscope (MRC-1024, Bio-Rad). We usually obtained 60–70% transfection efficiency, except for pEGFP-Mp85 βPIX (mutant type, S525A/T526A) of ~30%, as determined by counting the number of fluorescence positive cells relative to the total number of cells per field (×200).

Inhibition of p85 βPIX Phosphorylation by Protein Kinase Inhibitors—PC12FW cells were pre-treated with the following various inhibitors: PD98059 (50 μM), staurosporine (200 nM), K-252a (200 nM), LY294002 (50 μM), calphostin C (2 μM) or KN-62 (10 μM) for 1 h and stimulated with 10 ng/ml bFGF for 1 h. At the end of the incubation period, cells were washed in ice-cold PBS and solubilized in lysis buffer. The lysates were boiled for 5 min, resolved by 8% SDS-PAGE, and transferred to a PVDF membrane. Mobility shift of p85 βPIX on electrophoresis was detected by immunoblotting with anti-p85 βPIX antibody.

Dephosphorylation of p85 βPIX by Phosphatases—PC12FW cells were starved in serum-free DMEM containing doxycycline for 24 h. They were then stimulated with 10 ng/ml bFGF for 1 h and solubilized in lysis buffer. Cell lysates were incubated with alkaline phosphatase (25- 100 units/100 μl) and protein phosphatase 2A (2 units/100 μl) in dephosphorylation buffer (50 mM Tris-HCl, 0.1 mM EDTA, pH 8.5, 10 μg/ml aprotinin, and 10 μg/ml leupeptin) for 30 min at 30 °C. The reaction was terminated by adding 2× SDS-PAGE sample buffer, followed by immunoblotting with anti-p85 βPIX antibody.

PAK2 Assay—PC12FW cells were stimulated with 10 ng/ml bFGF for the indicated times and lysed in the lysis buffer described under "Metabolic Labeling." Cell lysates were immunoprecipitated with anti-PAK2 antibody. Immunoprecipitated PAK2 was incubated in kinase buffer (50 mM HEPES, pH 7.5, 10 mM $MgCl_2$, 2 mM $MnCl_2$, 0.2 mM dithiothreitol, and 100 μM ATP) containing 5 μg of myelin basic protein (MBP) and 10 μCi of [γ-^{32}P]ATP for 30 min at 30 °C. The reaction was terminated by adding 2× SDS-PAGE sample buffer. Phosphoproteins were resolved by 10% SDS-PAGE, transferred to a PVDF membrane, and exposed to x-ray film.

In Vitro Binding—GST and His-tagged PAK1 and PAK2 proteins were expressed in *E. coli* (DH5α and M15) according to the manufacturer's instruction, respectively. Equal amounts of GST or GST-ERK1 beads were incubated with bacterial lysates containing PAK1-His or PAK2-His for 1 h at room temperature in the lysis buffer described under "Metabolic Labeling." The beads were washed with the lysis buffer, resuspended in 2× SDS-PAGE sample buffer, boiled for 5 min, and then resolved by 10% SDS-PAGE. The gel was transferred to a PVDF membrane and immunoblotted with anti-His or anti-GST antibodies.

Immunoprecipitation and Immunoblotting—Cells were washed twice with PBS and lysed in the same lysis buffer described under "Metabolic Labeling" for 1 h at 4 °C. Proteins were immunoprecipitated with each antibody for 3 h at 4 °C. The immunoprecipitates were collected by addition of protein A- or G-Sepharose and washed 5 times with lysis buffer and 2 times with PBS. Samples were fractionated by SDS-PAGE and transferred to a PVDF membrane in a Tris/glycine/methanol buffer (25 mM Tris-base, 200 mM glycine, 20% methanol). Membranes were blocked with 3% skim milk in PBS for 1 h, incubated with primary antibodies for 1 h at room temperature, and then washed 3 times (10 min each) with PBS containing 0.1% Tween 20. Membranes were blotted with secondary horseradish peroxidase-conjugated antibodies for 1 h at room temperature. After 5 washes with PBS and 0.1% Tween 20, signals were detected using ECL reagent (Amersham Biosciences). In some cases, membranes were stripped and reprobed with different antibodies.

RESULTS

Establishment of an in Vitro PC12 Cell Line Model in Which Differentiation Is Accelerated by bFGF Stimulation—To investigate the molecular mechanism of bFGF-induced neuronal differentiation, we established a model system using PC12

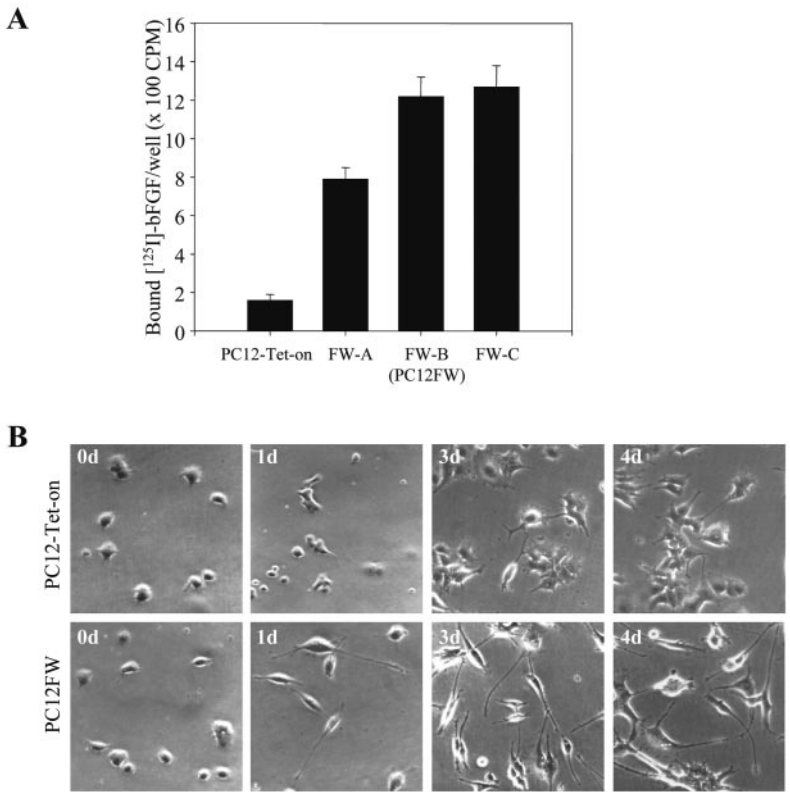

FIG. 1. **Inducible expression of FGFR-1 and its effect on the bFGF-induced morphological differentiation of PC12 cells.** *A*, parental PC12-tet-on cells and PC12 cells (*FWs*) overexpressing FGFR-1 were incubated in the receptor binding assay buffer containing ^{125}I-labeled bFGF for 3 h at 4 °C. Expression levels of FGFR-1 were measured as described under "Experimental Procedures." The FW-B clone was selected for further study and designated *PC12FW*. *B*, the morphological changes in parental PC12-tet-on cells and PC12FW cells during differentiation are compared. Both cells were grown on DMEM with 10% FBS (Tet system-approved FBS). To induce FGFR-1 expression, PC12FW cells were starved for 1 day in serum-free DMEM in the presence of 1.5 μg/ml doxycycline. The culture medium was then replaced by DMEM containing 10% FBS plus 10 ng/ml bFGF and changed every 48 h. At the indicated times, the cells were photographed under a phase contrast inverted microscope (magnification, ×200).

cells. Although parental PC12 cells have been widely used as a model system for differentiation, it has several drawbacks. For instance, it generally takes 5–7 days to observe the fully differentiated phenotype induced by bFGF. Thus, we made PC12 cell lines that overexpress the FGFR-1 upon induction by tetracycline (doxycycline). By the criterion of the receptor binding assay, a stable cell line (*FW-B* in Fig. 1, designated *PC12FW*) whose expression levels of FGFR-1 are 12 times as high as those of parental PC12-tet-on cells (Clontech) was selected for further analysis (Fig. 1*A*). Both PC12-tet-on cells and PC12FW cells in the absence of doxycycline have a similar small round shape (Fig. 1*B*). However, following doxycycline-induced overexpression of FGFR-1 and subsequent exposure to bFGF for 1 day, PC12FW cells exhibit morphological changes comparable with those of PC12-tet-on cells treated for 3–4 days, indicating that neurite extension is accelerated much more than in control PC12-tet-on cells. At the end of day 1 numerous PC12FW cells are already spindle shaped and have extended neurites whose length is ~2-fold greater than that of cell body. With further bFGF treatment PC12FW cells present conspicuous neurite elongation and form a neural network on days 3–4. In contrast, the neurites of PC12-tet-on cells at days 3–4 are still irregularly shaped and short. Fully developed neurites were observed after longer exposure (>1 week) (data not shown). These results demonstrate that PC12FW cells can serve as a highly efficient model system to elucidate the bFGF signaling pathway for neuronal differentiation.

Basic FGF Induces p85 βPIX Phosphorylation—Phosphorylation of GEFs such as Vav and Tiam-1 in response to extracellular stimuli is an important mechanism by which they are activated for cellular functions (49, 50). Evidence indicates that p85 βPIX also exists as a phosphoprotein (21), suggesting that p85 βPIX might be activated through phosphorylation in a similar manner. Thus, we determined whether bFGF induces p85 βPIX phosphorylation. PC12FW cells were metabolically labeled with [^{32}P]orthophosphate and then immunoprecipitated with anti-p85 βPIX antibody. As illustrated in Fig. 2*A*, a strongly labeled band migrating at 85 kDa was observed only in immunoprecipitates from bFGF-stimulated cells (*lane 3*). Correspondingly, the mobility of this band was slower than that of the p85 βPIX from unstimulated cells (*lane 2*). Several bands unidentified as yet were also observed, suggesting that other proteins might be associated with the p85 βPIX complex. We next examined the dose- and time-dependent response of bFGF-induced p85 βPIX phosphorylation. Cells were serum-starved and induced to overexpress FGFR-1 by treatment with doxycycline for 24 h. They were then stimulated with bFGF, and lysates were Western-blotted. Basal levels of weak phosphorylation were observed, as determined by the presence of a slowly migrating p85 βPIX band, even when cells were not stimulated (Fig. 2*B*). Basic FGF stimulates an upward shift in the mobility of p85 βPIX, which appears early, at 15 min. The levels of this band reach a peak at 1 h, are sustained until 4 h, and thereafter gradually decline over 24 h. This p85 βPIX mobility shift is detectable at concentrations of 5 ng/ml bFGF and is maximal at 50 ng/ml (Fig. 2*C*).

To confirm that the bFGF-induced shift of p85 βPIX is caused by phosphorylation, cell lysates were treated with alkaline phosphatase, a nonspecific phosphatase, and were subjected to Western blot analysis with anti-p85 βPIX antibody. When cells were stimulated with bFGF, as shown in Fig. 2*B*, a more slowly migrating form of p85 βPIX appears (Fig. 2*D*, *lane 2*). With increasing concentrations of alkaline phosphatase, the intensity of the upper band correspondingly decreases (*lanes 3–5*). These results indicate that p85 βPIX indeed migrates slowly due to phosphorylation. Next, to determine whether bFGF-dependent phosphorylation of p85 βPIX is primarily on tyrosine or serine/threonine residues, cell lysates were treated with protein phosphatase 2A, which dephosphorylates only phosphoserines and phosphothreonines. Treatment with protein phosphatase 2A, as with alkaline phosphatase, causes a similar change in the intensity of the upper phosphorylated band of p85 βPIX (Fig. 2*E*). However, genistein pretreatment does not have any significant effect on this shift (data not

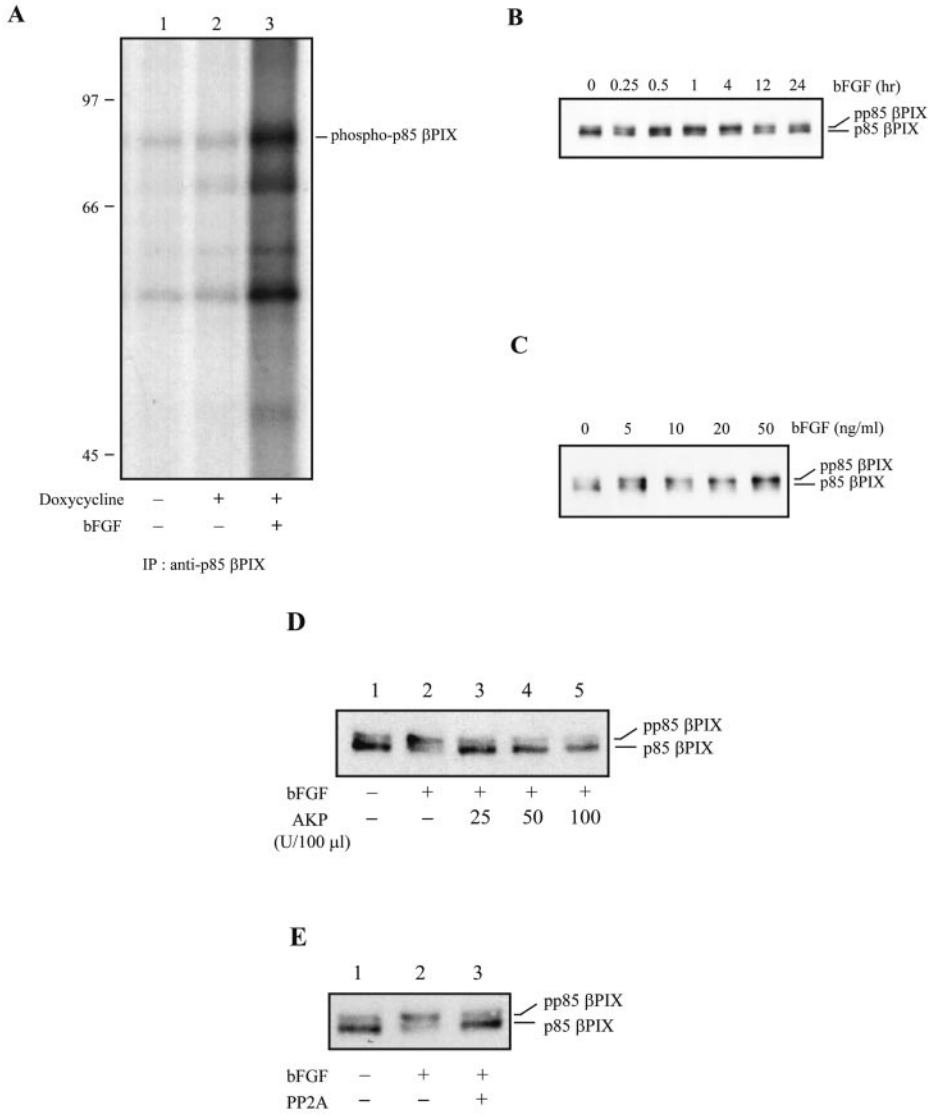

FIG. 2. **Basic FGF stimulates the phosphorylation of p85 βPIX on multiple serine/threonine residues.** *A*, autoradiogram of phosphorylated p85 βPIX. PC12FW cells were starved for 20 h in phosphate-free DMEM containing 1.5 μg/ml doxycycline to induce overexpression of FGFR-1 and incubated with 0.3 mCi/ml [^{32}P]orthophosphate in the absence (*lane 2*) or presence (*lane 3*) of 10 ng/ml bFGF for 4 h. [^{32}P]Orthophosphate-labeled p85 βPIX was immunoprecipitated with anti-p85 βPIX antibody, separated by 8% SDS-PAGE, and detected by autoradiography. *B* and *C*, time- and dose-dependent mobility shift of p85 βPIX. PC12FW cells were stimulated with 10 ng/ml bFGF for the indicated times (*B*) or incubated with the indicated concentrations of bFGF for 1 h (*C*). Cell lysates were resolved by 8% SDS-PAGE and immunoblotted with anti-p85 βPIX antibody. *D* and *E*, PC12FW cells were starved in serum-free DMEM containing doxycycline for 24 h and then treated with 10 ng/ml bFGF for 1 h. Equal amounts of proteins were incubated with the indicated concentrations of alkaline phosphatase (*D*) or protein phosphatase 2A (2 units/100 μl) (*E*) in a dephosphorylation buffer for 30 min. The reaction was terminated by the addition of SDS sample buffer. The reaction mixture was subjected to 8% SDS-PAGE analysis and immunoblotted with anti-p85 βPIX antibody.

shown). These results indicate that the bFGF-induced mobility shift of p85 βPIX is due to phosphorylation on multiple serine/threonine residues.

p85 βPIX Is Phosphorylated via the Ras/ERK Cascade—To identify the signaling pathway for bFGF-induced p85 βPIX phosphorylation, we used several inhibitors as follows: PD98059, a specific inhibitor of MEK; staurosporine and K-252a, broad spectrum inhibitors of protein kinases; LY294002, a specific inhibitor of PI3-kinase; calphostin C, a specific inhibitor of protein kinase C; and KN-62, a selective inhibitor of CaM kinase II. Cells were pretreated with each inhibitor for 1 h prior to stimulation with bFGF, and then alterations in the electrophoretic mobility of p85 βPIX were examined. The upward shift of p85 βPIX is suppressed by PD98059, staurosporine, or K-252a but not by LY294002, calphostin C, or KN-62 (Fig. 3*A*). Although staurosporine or K-252a affects the mobility of p85 βPIX, calphostin C (a specific protein kinase C inhibitor) does not. This might be due to a nonspecific effect of staurosporine or K-252a on the intermediate kinase(s) that functions upstream of p85 βPIX. An inhibitory effect of PD98059 on the shift is dose-dependent (Fig. 3*B*). PD98059 at 50 μM almost completely blocks the bFGF-induced shift. These results suggest that the Ras/ERK cascade pathway specifically regulates p85 βPIX phosphorylation. To confirm the specificity of the ERK pathway on the p85 βPIX mobility shift, a plasmid (pTM-MEK-S218A/S222A) encoding a dominant negative form of MEK1 was introduced. Expression of dominant negative MEK1 significantly attenuates the bFGF-induced phosphorylation of ERK1/2 (Fig. 3*C*, *lane 4* on the *bottom panel*). Under these conditions the intensity of the upper slowly migrating p85 βPIX band returns to the basal unstimulated level (*top panel*), indicating that the phosphorylation of p85 βPIX is downstream of MEK activity. We further determined whether Ras acts upstream of MEK in this signaling pathway by using a stable cell line (PC12DN-Ras) that expresses dominant negative Ras (N17 Ras) in a doxycycline-dependent manner. Expression of dominant negative Ras and its effect are evident as determined by the inhibition of the bFGF-induced activation of ERK1/2 (Fig. 3*D*, *bottom panel*). Basic FGF treatment results in the appearance of the slowly migrating form of p85 βPIX, indicating that p85 βPIX is phosphorylated (*lane 2*). However, when the expression of dominant negative Ras is induced by doxycycline, the bFGF-induced shift in the mobility of p85 βPIX is abolished (*lane 4*). Taken together, these results indicate that bFGF-induced p85 βPIX phosphorylation is mediated via the Ras/ERK cascade.

PAK2 Acts Downstream of ERK in p85 βPIX Phosphorylation—It has been reported (21) that PAK is an upstream kinase of p85 βPIX. From the observation that the bFGF-induced shift in the mobility of p85 βPIX is restored by pretreatment with

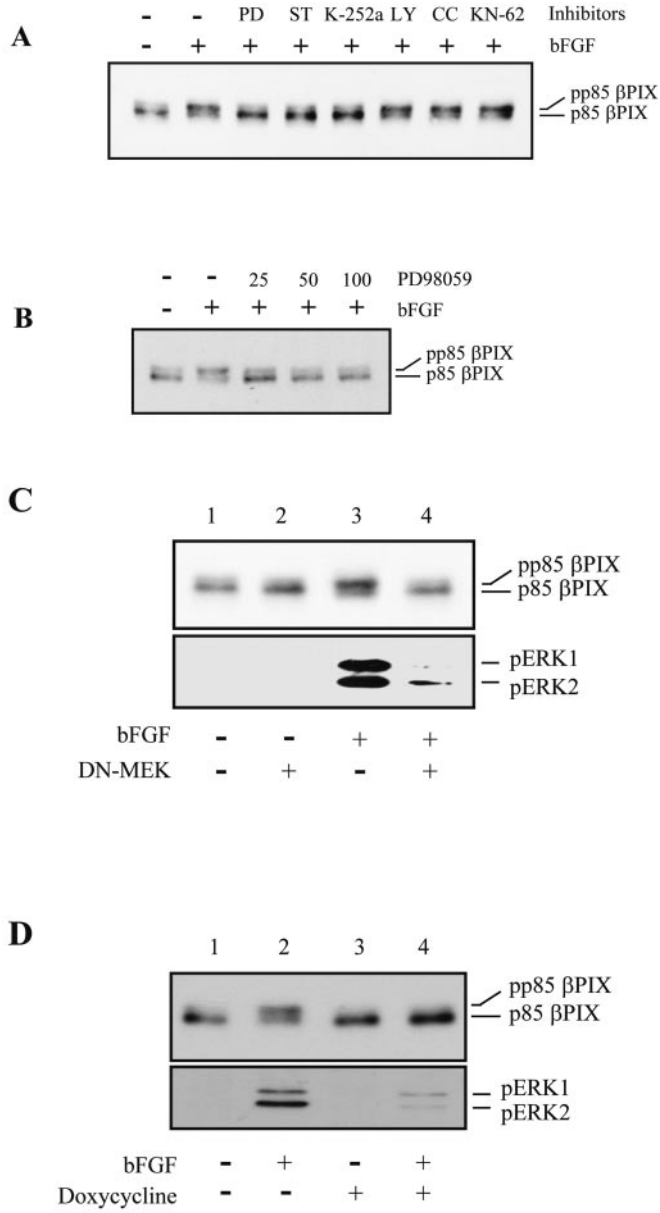

FIG. 3. **The signal pathway of bFGF-induced p85 βPIX phosphorylation.** *A* and *B*, PC12FW cells were pretreated with PD98059 (50 μM), staurosporine (200 nM), K-252a (200 nM), LY294002 (50 μM), calphostin C (2 μM), or KN-62 (10 μM) (*A*) or with the indicated concentrations of PD98059 for 1 h at 37 °C (*B*). Cells were then stimulated with 10 ng/ml bFGF for 1 h. Inhibition of the electrophoretic mobility shift of p85 βPIX was analyzed by immunoblotting with anti-p85 βPIX antibody. *C* and *D*, cells were transiently transfected with a plasmid encoding a dominant negative form of MEK1 (*DN-MEK*) using LipofectAMINE 2000 (*C*), or stable transfectants (PC12DN-Ras) expressing dominant negative Ras in a doxycycline-inducible manner were used (*D*). Phosphorylation of p85 βPIX was analyzed as described above (*top*). ERK activation was analyzed by immunoblotting with anti-phospho-specific ERK1/2 antibody, which specifically recognizes active ERK (*bottom*).

staurosporine or K-252a (Fig. 3*A*), we speculated that an unidentified target of these inhibitors might be PAK. We therefore postulate PAK as the kinase that links ERK and p85 βPIX. First, to determine which PAK isoform is dominantly expressed in PC12 cells, immunoprecipitation and immunoblotting were conducted using specific antibodies against each PAK (PAK1–3). PAK2 was identified as a major isoform (data not shown), consistent with the previous result (26). To test whether PAK2 is activated in response to bFGF, a kinase assay was performed using MBP as a substrate. PAK2 activity reaches a peak at 15 min following bFGF treatment, 3.5-fold higher than that of the control and returns to a basal level at 1 h (Fig. 4*A*). Immunoblotting with anti-PAK2 antibody shows that similar amounts of PAK2 were immunoprecipitated for the kinase reaction. We next determined whether bFGF-induced PAK2 activation is relevant for p85 βPIX phosphorylation. PAKs including PAK2 have an autoinhibitory domain (PID), which overlaps in part with the p21-binding domain in their N-terminal regulatory domain. PID binds to and negatively regulates the PAK activity (51). A GST-PID fusion form thus has been employed successfully to inhibit PAK activity *in vitro* and *in vivo* (51). Under the same principle we constructed a plasmid (pEGFP-PID) encoding GFP-PID fusion protein, whose expression can be easily monitored under a fluorescence microscope. Cells were transfected with this plasmid, and its effect on PAK2 activity was evaluated (Fig. 4*B*). Basic FGF stimulates PAK2 activation (*top*, *lane 2*), which is efficiently blocked by expression of GFP-PID (*lane 4*), validating the inhibitory effect of GFP-PID. Similar amounts of PAK2 were immunoprecipitated (*middle*) and GFP and GFP-PID are expressed at similar levels (*bottom*). We undertook the same approach to test whether PAK2 is a mediator of p85 βPIX phosphorylation. In the control pEGFP-transfected cells bFGF stimulates an upward shift of the p85 βPIX band (Fig. 4*C*, *top*, *lanes 1* and *2*). However, expression of GFP-PID returns this retarded mobility to that seen in unstimulated cells (*lanes 3* and *4*). Interestingly, inhibition of PAK2 activation by expression of GFP-PID does not influence bFGF-induced ERK activation (*bottom*, *lanes 2* and *4*), which is consistent with a previous report (25) that PAK does not act upstream of ERK in PC12 cells. These results indicate that PAK2 indeed functions upstream of p85 βPIX in the bFGF signaling pathway. Furthermore, although a number of studies have demonstrated that PAK acts upstream of MAPK in a variety of responses (22), our results suggest that ERK may act upstream rather than downstream of PAK2. To determine whether this is the case, we measured PAK2 activity in the presence of PD98059 or following transfection with pTM-MEK-S218A/S222A encoding a dominant negative form of MEK1 (DN-MEK). Basic FGF treatment induces a 3.8-fold increase in PAK2 activity (Fig. 5*A*), which is consistent with the result described above in Fig. 4*A*. PD98059 pretreatment results in the inhibition of the PAK2 activity by 60% (*lane 3*). Expression of DN-MEK also causes down-regulation of bFGF-stimulated PAK2 activation in similar levels (*lane 5*). These results support the idea that PAK2 activation is downstream of ERK. To resolve further the above issue we undertook another approach. Cells were transfected with pCMV6 (empty vector), pCMV6-PAK1 (T423E) encoding active Myc-PAK1, or pCMV6-PAK2 (T402E) encoding active Myc-PAK2, and then p85 βPIX phosphorylation and ERK activation were examined. Expression of active PAK1 or PAK2 results in p85 βPIX phosphorylation as determined by the retarded mobility of p85 βPIX, a change that is comparable with that induced by bFGF in cells transfected with an empty vector (Fig. 5*B*, *top*). However, active PAK1 or PAK2 does not affect ERK activation (*middle*, *lanes 3* and *4*). These results indicate that both PAK1 and PAK2 do not act upstream of ERK in PC12 cells. We next determined whether ERK and PAK2 form a complex. To this end, immunoprecipitation and Western blotting were performed. As shown in Fig. 5*C*, anti-PAK2 immunoprecipitate contains ERK1 and ERK2 (*lanes 1* and *2*). Conversely, anti-ERK immunoprecipitate reveals the presence of PAK2 (*lanes 3* and *4*). p85 βPIX can be seen in immunoprecipitates with either anti-PAK2 or anti-ERK, supporting the idea that ERK is indeed a constituent of the previously known PAK2-PIX com-

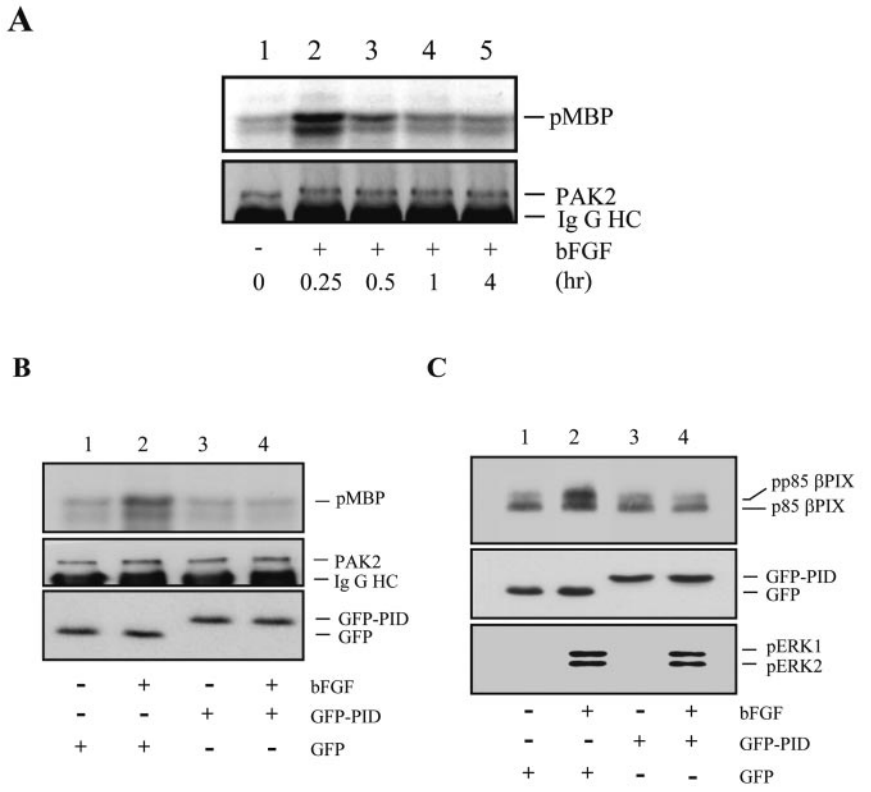

FIG. 4. **p85 βPIX phosphorylation is PAK2-dependent.** *A*, basic FGF stimulates activation of PAK2 in PC12FW cells. Cells were treated with 10 ng/ml bFGF for the indicated times at 37 °C. Cell lysates were then immunoprecipitated with anti-PAK2 antibody. Immunoprecipitated PAK2 was incubated with MBP and [γ-^{32}P]ATP in kinase assay buffer and subjected to SDS-PAGE analysis. Phosphorylated MBP was visualized by autoradiography (*top*). To monitor equal loading of PAK2, immunoblotting with anti-PAK2 antibody was performed (*bottom*). *B*, PC12FW cells were transiently transfected with pEGFP (control) or pEGFP-PID. Twenty four h after transfection cells were incubated for 1 h in the absence or presence of 10 ng/ml bFGF. Lysates were then processed as described above in *A* for PAK2 kinase assay. Phosphorylated MBP was visualized by autoradiography (*top*). Immunoblotting with anti-PAK2 antibody for equal loading of PAK2 (*middle*) or with anti-GFP antibody for expression of GFP and GFP-PID (*bottom*) was performed. *C*, PC12FW cells were transfected and processed as described above in *B*. Phosphorylation of p85 βPIX (*top*), expression of GFP and GFP-PID (*middle*), and ERK activation (*bottom*) were analyzed by immunoblotting with anti-p85 βPIX, anti-GFP, and anti-phospho-specific ERK antibodies, respectively.

plex. However, these interactions are independent of bFGF stimulation. To confirm that ERK, PAK2, and p85 βPIX are constitutively associated, pMyc-PAK1 (wild type PAK1) or pEGFP-PAK2 (wild type PAK2) was introduced into PC12FW cells, followed by immunoprecipitation and blotting analysis. Results similar to those illustrated in Fig. 5*C* were obtained from pEGFP-PAK2-transfected cells (Fig. 5*D*, *lanes 3* and *4*). However, PAK1 forms a complex only with p85 βPIX but not with ERK (*lanes 1* and *2*). Because these results strongly suggest that ERKs may directly bind to PAK2, we tested whether ERK1 and PAK2 bind *in vitro* using purified ERK1 and bacterially expressed PAK2. GST beads co-precipitated with neither PAK1-His nor PAK2-His (Fig. 5*E*, *middle*, *lanes 1* and *3*). In contrast, GST-ERK1 beads associated with PAK2-His but not with PAK1-His (*lanes 2* and *4*). Thus, PAK2 can play a role in linking ERK to p85 βPIX. We next determined which portion of PAK2 is responsible for its specific binding with ERK1. Because the *in vitro* binding study indicates that only PAK2 shows direct interaction with ERK1, and the amino acid sequences for the C-terminal kinase domains of PAK1 and PAK2 are highly homologous, our speculation is that the N terminus of PAK2 might be involved in binding. To test this idea, we generated a PAK2 deletion construct (amino acids 1- 327) encoding the N-terminal regulatory domain and an initial part of kinase domain to maintain the structural integrity. We then transfected two constructs for this deletion form and full-length PAK2 into PC12FW cells and determined whether they specifically bind to GST-ERK1 using GST pull-down assay. As shown in Fig. 5*F*, both short deleted and full-length PAK2 bind to ERK1 (*lanes 2* and *4*), suggesting that the N-terminal regulatory domain is essential for binding with ERK1. Collectively, these results suggest that the bFGF-induced phosphorylation of p85 βPIX is achieved via the ERK/PAK2 pathway and that phosphorylation depends on the formation of a multimeric complex consisting of ERK-PAK2-p85 βPIX.

Translocation of the p85 βPIX Complex to the Lamellipodia at Growth Cones Is Both ERK- and PAK2-dependent—It has been reported that the p85 βPIX-PAK complex co-localizes in the lamellipodia or membrane ruffle (21, 38). It was therefore assumed that the ERK/PAK2-dependent phosphorylation of p85 βPIX plays a role in the relocalization of this complex. We first determined whether targeting of the p85 βPIX-PAK complex is regulated in a bFGF stimulus-dependent manner. To monitor both expression and localization of p85 βPIX, we made a plasmid construct encoding p85 βPIX fused to the fluorescent protein GFP (GFP-p85 βPIX). Expression and localization of these proteins were analyzed by laser confocal microscopy. Cells underwent differentiation for 48 h prior to transfection of plasmids encoding GFP-p85 βPIX and GFP as a control. When cells are cultured in the absence of bFGF, diffuse staining is seen (Fig. 6*A*, *a* and *e*). In cells expressing GFP-p85 βPIX and treated with bFGF, strong bright fluorescence can be seen concentrated at the lamellipodia of growth cones, which resemble nascent sprouts (*b* and *c*). Furthermore, when bFGF is reintroduced into cells deprived of bFGF for 48 h starting from the transfection, a similar fluorescent pattern of multiple sprouts reappears (*d*). In control pEGFP-transfected cells, however, no such changes are observed (*f* and *g*). These results indicate that p85 βPIX is translocated to the lamellipodia at growth cones in response to bFGF. Because our co-immunoprecipitation data showed that PAK2-p85 βPIX association is not significantly affected by bFGF stimulation (Fig. 5*C*), we examined whether the translocated p85 βPIX at growth cones co-localizes with PAK2. PC12FW cells were co-transfected with pDS-Red-p85 βPIX and pEGFP-PAK2, which encode red fluorescent protein-p85 βPIX and GFP-PAK2, respectively. In the absence of bFGF, growth cone-like structures do not form at the tip of extending neurites (Fig. 6*B*, *a–c*). In contrast, bFGF treatment causes not only growth cones to form but also both red (p85 βPIX) and green (PAK2) fluorescence to specifically localize to these sites. Merged images show that p85 βPIX and PAK2 are almost identically distributed (Fig. 6*B*, *f*). Particu-

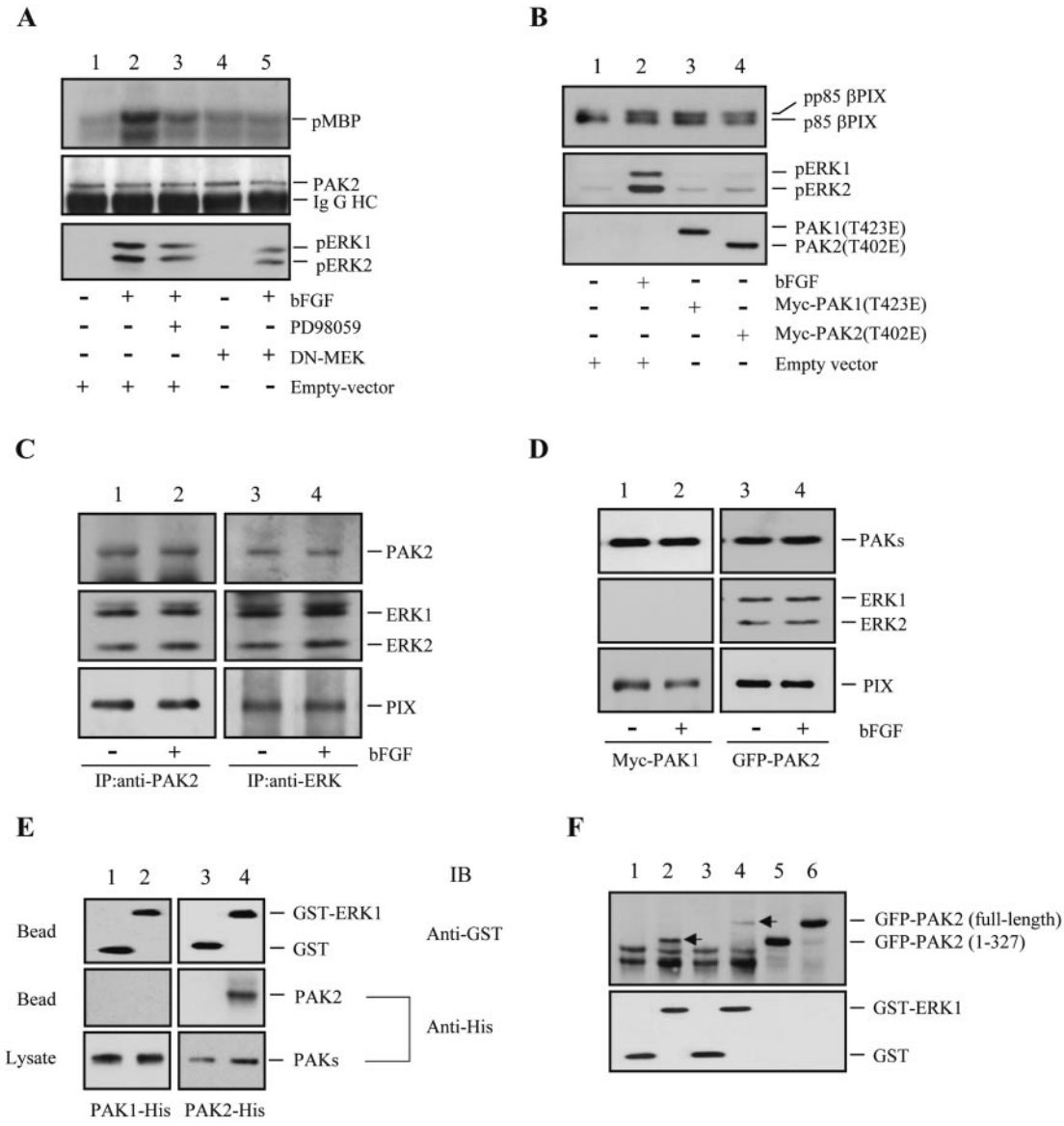

FIG. 5. **PAK2 activation is ERK1/2-dependent.** *A*, PC12FW cells were pretreated with 50 μM PD98059 for 1 h or transfected with a plasmid encoding a dominant negative form of MEK1 (*DN-MEK*) prior to stimulation with 10 ng/ml bFGF. Phosphorylated MBP was visualized by autoradiography (*top*). Immunoblotting with anti-PAK2 (*middle*) and anti-phospho-specific antibodies (*bottom*) was performed to confirm equal loading of PAK2 and to monitor the inhibitory effect of PD98059 and DN-MEK, respectively. *B*, control pCMV6 (*empty vector*), pCMV6-PAK1 for active Myc-PAK1 (T423E), or pCMV6-PAK2 for active Myc-PAK2 (T402E) was transiently introduced into PC12FW cells. Lysates were subjected to SDS-PAGE, and immunoblotting was then conducted with anti-p85 βPIX (*top*), anti-phospho-specific ERK (*middle*), and anti-Myc antibody (*bottom*), respectively. *C*, ERK is associated with the p85 βPIX-PAK2 complex. Cells were either unstimulated or stimulated with 10 ng/ml bFGF and then immunoprecipitated with anti-PAK2 (*lanes 1* and *2*) or anti-total ERK antibodies (*lanes 3* and *4*). Immunoprecipitates were Western-blotted with anti-PAK2 (*top*), anti-total ERK (*middle*), and anti-p85 βPIX antibodies for equal loading (*bottom*), respectively. *D*, ERK specifically interacts with the p85 βPIX-PAK2 complex but not with the Myc-PAK1 complex. Cells were transfected with pCMV6-Myc-PAK1 (wild type PAK1) or pEGFP-PAK2 (wild type PAK2) and immunoprecipitated (*IP*) with anti-Myc (*lanes 1* and *2*) or anti-GFP antibodies (*lanes 3* and *4*). Immunoprecipitates were analyzed by Western blotting with anti-Myc or anti-GFP (*top*), anti-total ERK (*middle*), and anti-p85 βPIX antibodies (*bottom*), respectively. *E*, full-length PAK1 and PAK2 were expressed as His-tagged proteins in *E. coli*. Equal amounts of purified GST or GST-ERK1 bound to glutathione-Sepharose beads (20 μl) were mixed with bacterial lysates (50–100 μg) and rinsed with washing buffer extensively (1 ml, 10×). Beads and lysates were subjected to Western analysis with anti-GST or anti-His antibodies. *F*, full-length PAK2 and a short deletion form of PAK2 were expressed as GFP-fusion proteins in PC12FW cells. Equal amounts of purified GST or GST-ERK1 bound to glutathione-Sepharose beads (20 μl) were mixed with cell lysates (50–100 μg) and rinsed with washing buffer extensively (1 ml, 10×). Beads were subjected to Western analysis with anti-GFP or anti-GST antibodies.

larly interesting is that they co-localize to the lamellipodia at growth cones of developing neurites. These results support the previous observation that p85 βPIX and PAK2 do not dissociate upon bFGF stimulation and suggest that they rather move as a unit in response to bFGF and promote growth cone formation through the regulation of actin dynamics.

To determine whether p85 βPIX translocation is mediated via the activation of the ERK/PAK2 pathway, PC12FW cells were pretreated with PD98059 or co-transfected with pEGFP-PID plus pDS-Red-p85 βPIX prior to stimulation with bFGF. In the absence of PD98059, strong fluorescence of p85 βPIX was seen at growth cones. However, PD98059 pretreatment prevents p85 βPIX accumulation at the same location (data not shown). Basic FGF-induced translocation of red fluorescent protein-p85 βPIX is similar to that of GFP-p85 βPIX (Fig. 6*C*, *a* and *e*). When PAK2 is inhibited by the expression of GFP-

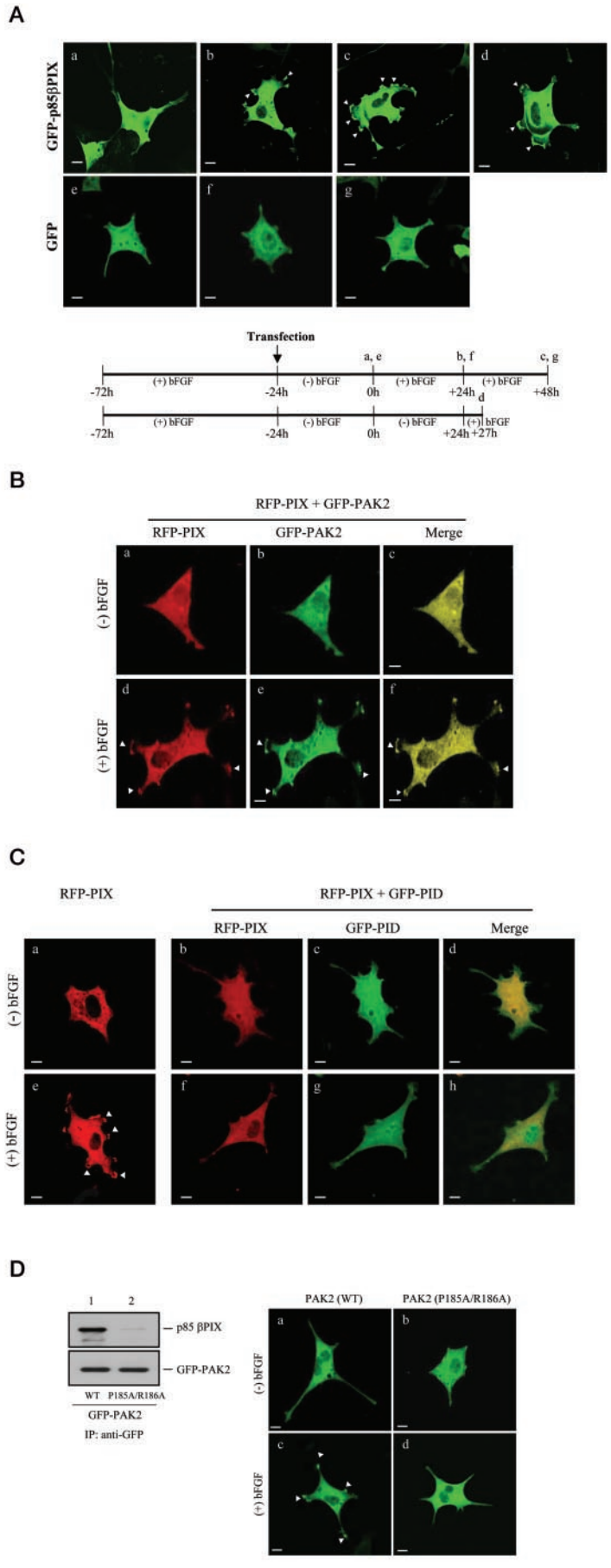

FIG. 6. **Translocation of the p85 βPIX complex during bFGF-induced differentiation.** *A*, PC12FW cells were cultured on poly-L-lysine-coated coverslips and induced to differentiate in complete medium containing 10 ng/ml bFGF for 48 h and then transfected with pEGFP (control) or pEGFP-p85 βPIX. Transfected cells were cultured in the absence of bFGF for 24 h. bFGF was reintroduced to the cells for the indicated times except for *d* in which bFGF deprivation continued for the next 24 h; cells were then stimulated for 3 h. Localization of green fluorescence for p85 βPIX was determined using laser confocal microscopy. Time schedule for transfection and bFGF treatment is shown at the *bottom*. *B*, cells were differentiated for 48 h in the presence of bFGF, and co-transfected with pDS-Red-p85 βPIX (wild type p85 βPIX) and pEGFP-PAK2 (wild type PAK2). Cells were then cultured in the absence or presence of 10 ng/ml bFGF for 24 h. To determine their respective patterns of localization, transfected cells expressing both p85 βPIX and PAK2 were selected and analyzed as described above. *C,* cells were differentiated for 48 h and then transfected with pDS-Red-p85βPIX only or pDS-Red-p85βPIX plus pEGFP-PID. 24 h after transfection, cells were left untreated or treated with 10 ng/ml bFGF for 24 h. Localization of fluorescence was determined as described above. Images show *red* fluorescence for p85 βPIX and *green* fluorescence for GFP-PID, respectively. Note the presence of green fluorescence in the periphery. *D*, mutant PAK2 (P185A/R186A) is defective in translocation to the lamellipodia at growth cones. PC12FW cells were transfected with pEGFP-PAK2 (wild type, *WT*) or pEGFP-MPAK2 (mutant type, P185A/R186A). Lysates were immunoprecipitated with anti-GFP antibody, followed by Western analysis with anti-p85 βPIX (*top*, *left*) or anti-GFP antibody (*bottom*, *left*). To assess translocation potential, cells were allowed to differentiate for 48 h and then transfected with a plasmid for either wild or mutant PAK2 (P185A/R186A). 24 h after transfection, cells were left untreated (*a* and *b*, *right*) or treated (*c* and *d*, *right*) with 10 ng/ml bFGF for 24 h at 37 °C. Localization of fluorescence was determined as described above. Representative images from more than three independent experiments are shown here. The *scale bar*, 10 μm.

PID, specific targeting of red fluorescence (p85 βPIX) to the lamellipodia at growth cones disappears (Fig. 6*C*, *b* and *f*). Instead, the cytoplasm diffusely stains red. This is more obvious in the merged picture where most of the cytoplasm stains *yellow,* representing the co-localization of PID and p85 βPIX, and the periphery stains *green*, representing the presence of only PID (Fig. 6*C*, *d* and *h*). These results indicate that the bFGF-induced translocation of p85 βPIX depends on the activity of both ERK and PAK2. To address further the issue whether PAK2-p85 βPIX binding is essential for translocation of this complex, we made a construct for the PAK2 mutant that is not able to bind to p85 βPIX. Because Pro-193 and Arg-194 in PAK1 are essential for binding with SH3 domain of PIX (52) and these two residues are conserved in PAK2, they were mutagenized to alanines. Expectedly, this mutant PAK2 (P185A/R186A) shows no significant binding to p85 βPIX compared with that of wild type PAK2 (Fig. 6*D*, *left*). We thus transfected the plasmids for wild and mutant PAK2 and compared their translocation capability. Accumulation of green fluorescence representing wild type PAK2 is shown at the neurite tips in response to bFGF (Fig. 6*D*, *a* and *c*). In contrast, mutant PAK2 is rarely observed at the similar area of neurites (Fig. 6*D*, *b* and *d*). Moreover, mutant PAK2-transfected cells frequently exhibit a morphological change, *i.e.* slender neurites with pointed ends, resembling those seen in cells whose growth cones retract in response to harmful stimuli. Taken together, these results suggest that PAK2 binding to p85 βPIX as well as PAK2-mediated activation of p85 βPIX are essential for targeting of this complex to the lamellipodia at growth cones.

p85 βPIX Phosphorylation Correlates with Its Translocation and Neurite Outgrowth—PAK2 activation correlates with both phosphorylation (Fig. 4*B*) and translocation (Fig. 6*C*) of p85 βPIX. It has been reported recently (39) that the major PAK1-mediated phosphorylation sites of p85 βPIX map to Ser-525 and Thr-526. Therefore, using a mutant p85 βPIX (S525A/T526A) whose serine 525 and threonine 526 residues are replaced by alanine, we examined by metabolic labeling whether PAK2-mediated p85 βPIX phosphorylation also takes place at these sites. PC12FW cells were transfected with pEGFP-p85 βPIX (wild type) or pEGFP-Mp85 βPIX (mutant type, S525A/T526A) prior to labeling of cells with [^{32}P]orthophosphate. Lysates were then immunoprecipitated with anti-GFP antibody. Wild type p85 βPIX shows basal levels of phosphorylation in unstimulated cells (Fig. 7*A*, *lane 1*). bFGF treatment causes an increase in p85 βPIX phosphorylation, which is consistent with data shown in Fig. 2*A*. In contrast, no band corresponding to wild type p85 βPIX was seen in cells transfected with pEGFP-Mp85 βPIX (Fig. 7*A*, *lanes 3* and *4*). Immunoblotting with anti-GFP reveals the expression of both wild type and mutant p85 βPIX (*bottom*). These results indicate that PAK2-mediated p85 βPIX phosphorylation also involves Ser-525 and Thr-526.

To determine whether p85 βPIX phosphorylation at Ser-525 and Thr-526 is functionally linked to translocation of the PIX complex and neurite outgrowth, we assessed whether mutant p85 βPIX could be properly targeted to the lamellipodia at growth cones, and we examined its effect on neurite outgrowth. In cells expressing wild type p85 βPIX (GFP-p85 βPIX), the protein localizes to the lamellipodia at growth cones following bFGF stimulation (Fig. 7*B*, *a* and *c*), which is consistent with the result shown in Fig. 6*A*. However, mutant p85 βPIX (GFP-p85 βPIX S525A/T526A) rarely accumulates at these locations (*b* and *d*), indicating that p85 βPIX phosphorylation at these two residues is critical for targeting of the p85 βPIX complex. Furthermore, we were unable to observe growth cone-like structures in cells expressing mutant p85 βPIX at higher levels. To test whether p85 βPIX phosphorylation is required for neurite outgrowth, we transfected PC12FW cells with a plasmid encoding either wild type or mutant p85 βPIX and assessed differentiation by neurite outgrowth. Wild type p85 βPIX promotes neurite formation at ~2-fold greater efficiency than does a GFP control (Fig. 7*C*, *bottom*). Cells expressing wild type p85 βPIX also extend numerous neurites (*top center*). In contrast, neurite extension is significantly blocked by the mutant p85 βPIX, at a level of half that of a GFP control. Cells expressing mutant p85 βPIX have deformed shapes with short neurites compared with surrounding untransfected cells, in which more than 70% are scored as differentiation positive (Fig. 7*C*, *top right*). These results suggest that p85 βPIX phosphorylation at the Ser-525 and Thr-526 residues mediates translocation of the p85 βPIX complex to the lamellipodia at growth cones and that disruption of this process results in an inhibition of neurite outgrowth induced by bFGF.

DISCUSSION

The role of the ERK pathway in neurite extension has been extensively studied in the PC12 cell model (53, 54). Upon stimulation by the growth factors such as bFGF and NGF, ERK is activated in a Ras- and a Rap1-dependent manner (55, 56), followed by translocation to the nucleus where it regulates transcriptional activity. Evidence indicates that in addition to the nuclear targets, ERK also activates a number of cytoplasmic proteins independent of nuclear signaling (57). Moreover, it has been shown that an artificially ERK2-MEK1 fusion protein strongly localizes to the extending processes of neurites (58), where p85 βPIX also accumulates during PC12 cell differentiation (Fig. 6). These results suggest that ERK action at the site of neurite extension is also as important as its activities in the nucleus and that its potential substrates might be the PAK2-p85 βPIX complex. In this respect, our discovery of the PAK2-p85 βPIX complex as a downstream mediator of ERK explains how bFGF promotes neurite outgrowth via the Ras/ERK cascade. It is noteworthy that the ERK cascade couples two important signaling pathways of Ras and PAK2 for PC12 cell neurite outgrowth. PAK2 is activated following bFGF treatment, and its activity is inhibited by PD98059 pretreatment or expression of dominant negative MEK1 (Figs. 4*A* and 5*A*). Phosphorylation of p85 βPIX is both ERK- and PAK2-dependent (Figs. 3 and 4*B*). Based on our observations and those from other laboratories (21, 25, 26), we therefore speculate that ERK first activates PAK2, which in turn phosphorylates p85 βPIX (summarized in Fig. 8). First, in our transfection study PAK2 immunoprecipitate contains ERK and p85 βPIX, whereas in the PAK1 immunoprecipitate only p85 βPIX is present (Fig. 5*D*). Because it has been well documented that both PAK1 and PAK2 bind p85 βPIX through their PIX-binding motif (P*XXX*P), this result strongly suggests that PAK2 but not PAK1 directly binds to ERK. Indeed, it has been confirmed by *in vitro* binding study (Fig. 5*E*). Furthermore, this physical interaction can also resolve the issue of how the ERK cascade specifically signals to this complex. Second, transfection studies with wild type and mutant PAKs in PC12 cells showed that PAK activation does not correlate with the activation of ERK and JNK, indicating that at least these MAPKs are not downstream of PAK1 (25) or PAK2. However, p85 βPIX is strongly phosphorylated by introduction of an active PAK1 or PAK2 (Fig. 5*B*), as determined by mobility shift, which is in agreement with a previous report that PAK phosphorylates p85 βPIX (21). Third, comparison of phosphopeptide maps of p85 βPIX obtained *in vivo* and *in vitro* (not shown) made it unlikely that p85 βPIX is a substrate of ERK.

PAK2 is regulated in a number of ways. During hyperosmolarity-induced apoptosis PAK2 is cleaved via a caspase-dependent mechanism, which releases the catalytically active C-ter-

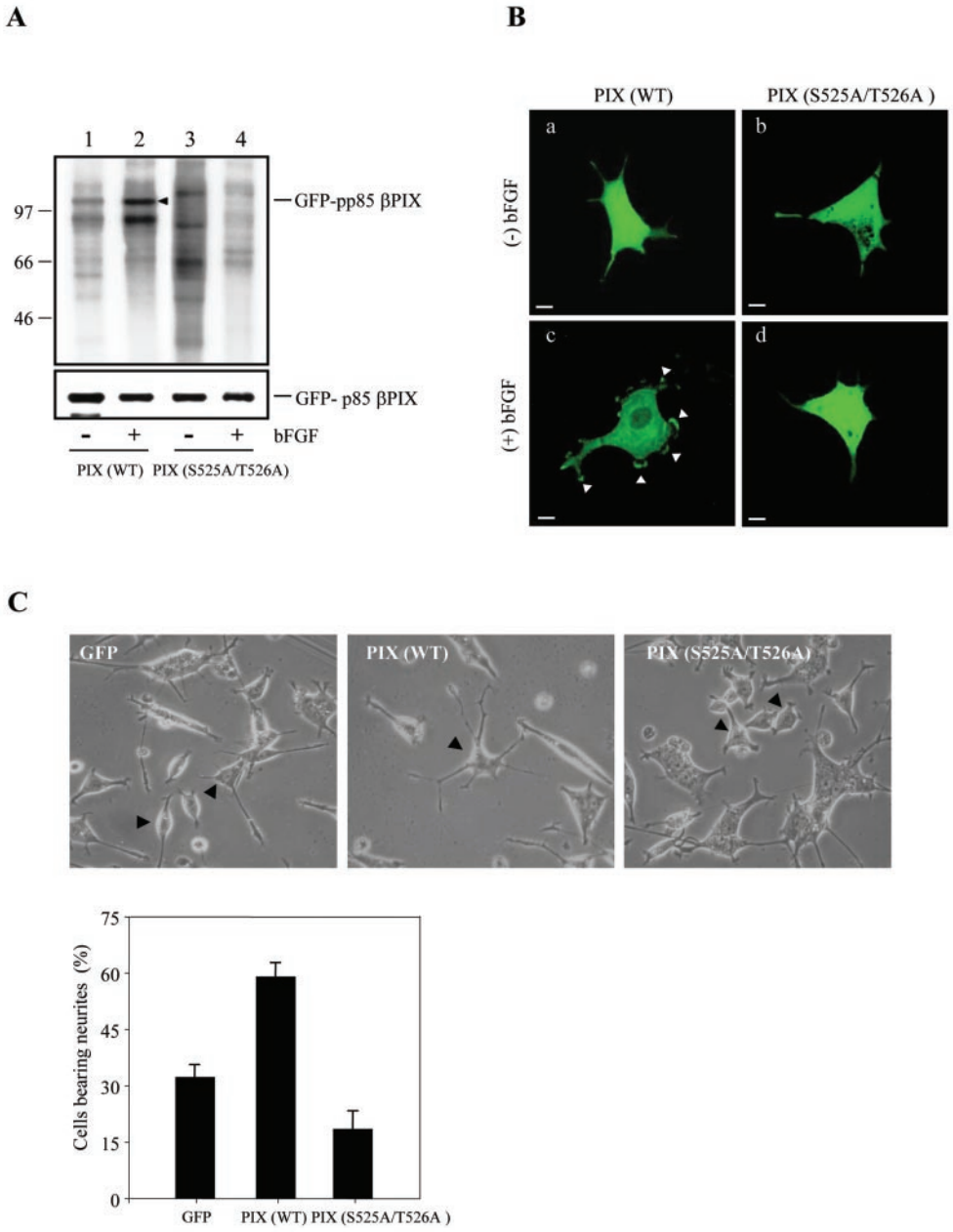

FIG. 7. **Defective translocation of mutant p85 βPIX (S525A/T526A) and its effect on neurite outgrowth.** *A*, mutant p85 βPIX is not metabolically labeled with [^{32}P]orthophosphate. PC12FW cells were transfected with pEGFP-p85 βPIX (wild type, *WT*) or pEGFP-Mp85 βPIX (mutant type, S525A/T526A). Cells were then processed as described in Fig. 2*A* except for immunoprecipitation with anti-GFP antibody. The immunoprecipitates were separated by 8% SDS-PAGE, transferred to a nylon membrane, and detected by autoradiography. To identify p85 βPIX, the same blot was probed with anti-GFP antibody, and the result was compared with that from autoradiography. *B*, mutant p85 βPIX is defective in translocation to the lamellipodia at growth cones. PC12FW cells were allowed to differentiate for 48 h and then transfected with pEGFP-p85 βPIX or pEGFP-Mp85 βPIX. 24 h after transfection, cells were left untreated (*top*) or treated (*bottom*) with 10 ng/ml bFGF for 24 h at 37 °C. Localization of fluorescence was determined as described above. *Bar*, 10 μm. *C*, mutant p85 βPIX inhibits bFGF-induced neurite outgrowth. PC12FW cells were transfected with pEGFP (control), pEGFP-p85 βPIX, or pEGFP-Mp85 βPIX. 24 h after transfection, cells were cultured for differentiation in complete medium containing 10 ng/ml bFGF for 48 h at 37 °C. Representative images of fluorescence micrographs were captured by the SPOT system (Diagnostic Instruments Inc., *top*). Typical cells expressing fluorescent proteins are marked (*arrowhead*). Inhibition of bFGF-induced neurite outgrowth was determined by comparing the percentage of differentiated cells with neurites longer than two body lengths in total green cells. Green cells in at least 10 different microscope fields of view were counted (>10 cells/field) (*bottom*). Values represent mean ± S.D. from three independent experiments.

minal kinase domain of PAK2 (59). Human immunodeficiency virus, type 1, Nef associates with and activates PAK2 (60, 61), which contributes to the pathogenicity of human immunodeficiency virus infection. Recently, it has been shown that c-Abl and PAK2 functionally interact (62). In this interaction PAK2-activated c-Abl down-regulates PAK2 activity, suggesting the existence of a negative feedback loop between these two proteins. The present study adds to the repertoire of PAK2 regulation through association with ERK. According to a model for PAK1 activation, multiple events are required for the full activation of inactive PAK1 (63). Phosphorylation of two conserved residues, Ser-144 and Thr-422, plays a key role in this process. Because Ser-141 and Thr-402 of PAK2 (analogous to Ser-144 and Thr-422 of PAK1, respectively) are well conserved, it appears that PAK2 is activated by a mechanism similar to that of PAK1 activation. Considering that ERK is a kinase that

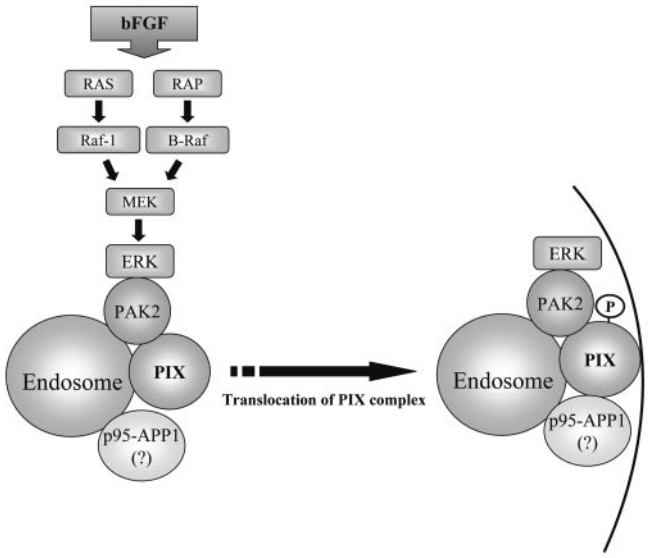

FIG. 8. **A model for the role of p85 βPIX in the bFGF signal transduction for neurite outgrowth.** Upon bFGF stimulation the Ras/ERK cascade pathway is activated. It has been suggested recently that the ERK cascade could also be activated in a Rap1-dependent manner, particularly for sustained activation of ERK in PC12 cells. Both ERK and PAK2 function upstream of p85 βPIX phosphorylation. Our observations suggest that ERK acts upstream of PAK2 by associating with the PIX complex in which p85 βPIX interacts with PAK2 and p95 family members. Although PAK2 is a direct upstream kinase for p85 βPIX, it is unlikely that ERK is also involved directly in p85 βPIX phosphorylation. Recent evidence indicates that PIX is required for the recruitment of p95-APP1 to the Rab11-positive endosomes (71). In this model we propose that p85 βPIX phosphorylation is a targeting signal for the PIX complex. Therefore, ERK and PAK2 activities are essential for this process. This idea is supported by the finding that inhibition of the activities of these two enzymes blocks not only translocation of the PIX complex but also bFGF-induced neurite outgrowth. However, PAK2 activity does not seem to be required for its action at the membrane. Phosphorylation-induced conformational changes in p85 βPIX may involve p95 family members (see text for details). At present it is not clear whether Rac1 or Cdc42 actively participates in translocation or simply acts as a passive binding partner through interaction with PAK at the membrane (26, 71).

acts immediately upstream of PAK2, ERK-mediated PAK2 phosphorylation may exert a major influence on PAK2 activation. The N-terminal regulatory domain functions to repress catalytic activity of PAK. Thus, conformational changes induced by caspase-mediated proteolytic release of or direct binding of various lipids to this region can relieve the repression (59, 64). Analogous to this activation mode, ERK-mediated PAK2 phosphorylation, presumably in the N-terminal regulatory domain, may induce a conformational change in PAK2, resulting in activation of PAK2. Binding of Rac1- or Cdc42-GTP to the p21-binding domain can also relieve the N terminal-mediated repression. In this case, ERK may contribute to the initial activation of PAK2, which remains in a partially active state, followed by the late activation step via interaction with Rac1- or Cdc42-GTP, which leads to full activation by transphosphorylation of Thr-402. Given this scenario, it is conceivable that in contrast to the negative feedback loop shown for the PAK2-c-Abl interaction, a positive feedback loop may operate for PAK2 activation in an ERK-PAK2 complex. However, the kinetics of PAK2 activation shows only a single peak at 15 min and not a second peak at a later stage (Fig. 4*A*). It has also been reported that growth factor-mediated Rac1-GTP is not responsible for activation of PAK (45), suggesting that there is no interaction between PAK2 in the PAK2-p85 βPIX complex and bFGF-mediated Rac1- or Cdc42-GTP. It is therefore likely that the late activation step mentioned above does not occur in bFGF-induced PAK2 activation. Alternatively, ERK may phosphorylate serine/threonine(s) in the kinase domain of PAK2. Indeed, multiple sites are compatible with an ERK consensus phosphorylation sequence of (S/T)P. An example for this activation mechanism is 3-phosphoinositide-dependent kinase 1 (PDK1)-mediated phosphorylation of PAK1 on threonine 422 in the activation loop of PAK1 (65). Because threonine 422 is masked by the regulatory domain in the inactive "closed" state, the activation loop of PAK1 should be exposed to PDK1 prior to phosphorylation by PDK1. Thus, PDK1 needs an accessory factor such as sphingosine to allow access to its substrate. In a similar manner ERK-mediated PAK2 phosphorylation may require a preceding event. Further studies are necessary to understand the mechanism by which PAK2 is activated by ERK.

It has been well documented that PAK plays a pivotal role in neurite outgrowth (25, 26). Recruitment of PAK to target sites, including growth cones in PC12 cells, is critical for its biological function. However, the mechanism whereby PAK is relocated has not been defined. Although Nck-mediated targeting of PAK1 to the membrane has been suggested as a potential mechanism for PC12 cell neurite outgrowth, this does not seem to be the case (26, 37). Another candidate molecule for PAK2 targeting is p85 βPIX. We demonstrated that PAK2 and p85 βPIX are constitutively associated and that their translocation to the lamellipodia at growth cones as monitored by the localization of fluorescent p85 βPIX (GFP-p85 βPIX) occurs in a bFGF-dependent manner (Fig. 6). In conjunction with the results from other laboratories, we thus propose a PIX adaptor model, in which we describe the role of p85 βPIX in bFGF-induced neuritogenesis (Fig. 8). In this p85 βPIX-mediated targeting model, PAK2 activation is essential for translocation of the PAK2-p85 βPIX complex. Inhibition of PAK2 activity by expression of PID causes retention of this complex in the cytosol (Fig. 6*C*). Furthermore, the mutant p85 βPIX (S525A/T526A) exhibits significant defect in targeting to the lamellipodia at growth cones (Fig. 7*B*). Consistent with this, bFGF-induced neurite extension is significantly blocked by expression of PID (data not shown) or of the mutant p85 βPIX (Fig. 7*C*). It has been reported that the affinity of PAK1 for PIX is regulated by PAK1 activation levels (45). The PAK1-PIX complex dissociates if PAK1 is autophosphorylated at Ser-198 and Ser-203, which promotes PAK1 cycling from the focal complex back to the cytosol. Our observations that PAK2 is still present in p85 βPIX immunoprecipitates and that PAK2 and p85 βPIX co-localize at growth cones following bFGF stimulation suggest that PAK2 may not be strongly activated to lose its affinity for p85 βPIX. Indeed, PAK2 activity increases 3–4-fold over basal levels in response to bFGF, whereas active GTP-bound Rac1 or Cdc42 induces PAK activation greater than 100-fold (63). In this regard PAK2 in the p85 βPIX complex may not be a downstream target of Rac1 or Cdc42. It is more likely that PAK2 and Rac1/Cdc42 behave independently and execute their specific functions by regulating different effectors. Alternatively, the affinity of PAK2 for p85 βPIX might be regulated in a way different from that of PAK1.

The next step, how PAK2-mediated p85 βPIX phosphorylation is translated into a targeting signal for this complex, remains unclear. Accumulating evidence indicates that phosphorylation of GEFs of the Dbl family on Ser/Thr and Tyr residues is important for GEF activities. The Dbl family PH domains are considered to regulate the GEF activity of the adjacent DH domains through phosphoinositide interaction and phosphorylation. In the inactive state the PH domain bound to phosphatidylinositol 4,5-phosphate contacts the DH domain, masking the Rac1-binding site and exerting an inhib-

itory effect on the GEF activity of the DH domain (66). In the presence of phosphatidylinositol 3,4,5-phosphate, a PI3-kinase product (67), and tyrosine phosphorylation by Src-related kinases (49), the constraint on the DH domain is relieved. The DH and PH domains of p85 βPIX, however, behave independently in solution, unlike the cognate domains of other Dbl family members (66), suggesting that the p85 βPIX DH domain is regulated somewhat differently. In this context Manser *et al.* (21) reported that PIX phosphorylation does not seem to correlate with the GEF activity of PIX toward Rac1, raising the possibility that another downstream target(s) is functionally relevant for PIX phosphorylation-mediated cellular functions. Recently, a family of proteins that interact with PIX through the GB domain has been discovered. p95-APP1, a member of this family, links the PIX complex to paxillin (68), which is a critical component of focal adhesion. Paxillin is phosphorylated by various stimuli including growth factors, and its phosphorylation is involved in targeting to focal adhesion (69) or cell migration (70). Our data (not shown) revealed the presence of phosphorylated paxillin in the p85 βPIX immunoprecipitate in response to bFGF. This has prompted us to speculate that because p85 βPIX phosphorylation is bFGF stimulus-dependent, phosphorylation-induced conformational changes in p85 βPIX may generate a new interaction between p85 βPIX and paxillin via p95-APP1, which results in recruitment of this complex to the lamellipodia at neuronal growth cones where Rac1-mediated organization of actin is actively underway (71). The data that Rac1 and p95-APP1 co-localize and Rac1 activity is required for p95-APP1-induced protrusions support this idea (68). Moreover, p95PKL, which shows a high degree of homology to p95-APP2 (99% identical at both the protein and nucleotide levels), also mediates recruitment of the PAK-PIX complex to focal adhesion through an association with paxillin LD4 motif. In this case activation of the adaptor function of PAK, presumably leading to PAK-induced PIX phosphorylation, is required for unmasking of p95PKL paxillin-binding subdomain 2 to bind to paxillin. In contrast, Zhao *et al.* (45) proposed that GIT1 promotes focal adhesion disassembly, which is not due to recruitment of PAK-PIX complex. This might be due to its unique ability to interact with FAK, which serves to facilitate focal complex turnover. Thus, utilizing distinct members of this family, cells can precisely regulate various cellular functions including cell adhesion and motility through focal adhesion dynamics. PC12 cells can regulate cytoskeletal reorganization required for neurite outgrowth in a similar way, which involves the precise temporal-spatial activation of the p85 βPIX complex and the p95 family members as its downstream effectors.

In conclusion, the present study provides evidence that the bFGF-induced phosphorylation of p85 βPIX is mediated through the Ras/ERK/PAK2 pathway and that this phosphorylation is the signal for recruitment of the PAK2-p85 βPIX complex to the lamellipodia at growth cones where PAK2 promotes neurite outgrowth by regulating actin dynamics. It seems likely that this signaling pathway is also involved in NGF-induced neuritogenesis. Further studies on the identification of the translocation machinery for this complex will provide more insight into the molecular mechanism of bFGF-induced neurite outgrowth.

REFERENCES

1. Zheng, Y. (2001) *Trends Biochem. Sci.* **26,** 724–732
2. Hall, A. (1998) *Science* **279,** 509–514
3. Mackay, D. J., Nobes, C. D., and Hall, A. (1995) *Trends Neurosci.* **18,** 496–501
4. Albertinazzi, C., Gilardelli, D., Paris, S., Longhi, R., and de Curtis, I. (1998) *J. Cell Biol.* **142,** 815–825
5. Brouns, M. R., Matheson, S. F., and Settleman, J. (2001) *Nat. Cell Biol.* **3,** 361–367
6. Lehmann, M., Fournier, A., Selles-Navarro, I., Dergham, P., Sebok, A., Leclerc, N., Tigyi, G., and McKerracher, L. (1999) *J. Neurosci.* **19,** 7537–7547
7. Tanabe, K., Tachibana, T., Yamashita, T., Che, Y. H., Yoneda, Y., Ochi, T., Tohyama, M., Yoshikawa, H., and Kiyama, H. (2000) *J. Neurosci.* **20,** 4138–4144
8. Luo, L., Liao, Y. J., Jan, L. Y., and Jan, Y. N. (1994) *Genes Dev.* **8,** 1787–1802
9. Lamoureux, P., Altun-Gultekin, Z. F., Lin, C., Wagner, J. A., and Heidemann, S. R. (1997) *J. Cell Sci.* **110,** 635–641
10. Kuhn, T. B., Brown, M. D., and Bamburg, J. R. (1998) *J. Neurobiol.* **37,** 524–540
11. Luo, L. (2000) *Nat. Rev. Neurosci.* **1,** 173–180
12. Kim, M. D., Kolodziej, P., and Chiba, A. (2002) *J. Neurosci.* **22,** 1794–1806
13. Jalink, K., van Corven, E. J., Hengeveld, T., Morii, N., Narumiya, S., and Moolenaar, W. H. (1994) *J. Cell Biol.* **126,** 801–810
14. Kranenburg, O., Poland, M., van Horck, F. P., Drechsel, D., Hall, A., and Moolenaar, W. H. (1999) *Mol. Biol. Cell* **10,** 1851–1857
15. Shamah, S. M., Lin, M. Z., Goldberg, J. L., Estrach, S., Sahin, M., Hu, L., Bazalakova, M., Neve, R. L., Corfas, G., Debant, A., and Greenberg, M. E. (2001) *Cell* **105,** 233–244
16. Altun-Gultekin, Z. F., and Wagner, J. A. (1996) *J. Neurosci. Res.* **44,** 308–327
17. Chen, X. Q., Tan, I., Leung, T., and Lim, L. (1999) *J. Biol. Chem.* **274,** 19901–19905
18. Kita, Y., Kimura, K. D., Kobayashi, M., Ihara, S., Kaibuchi, K., Kuroda, S., Ui, M., Iba, H., Konishi, H., Kikkawa, U., Nagata, S., and Fukui, Y. (1998) *J. Cell Sci.* **111,** 907–915
19. Goi, T., Rusanescu, G., Urano, T., and Feig, L. A. (1999) *Mol. Cell. Biol.* **19,** 1731–1741
20. Posern, G., Saffrich, R., Ansorge, W., and Feller, S. M. (2000) *J. Cell. Physiol.* **183,** 416–424
21. Manser, E., Loo, T. H., Koh, C. G., Zhao, Z. S., Chen, X. Q., Tan, L., Tan, I., Leung, T., and Lim, L. (1998) *Mol. Cell* **1,** 183–192
22. Dan, I., Watanabe, N. M., and Kusumi, A. (2001) *Trends Cell Biol.* **11,** 220–230
23. Manser, E., Leung, T., Salihuddin, H., Zhao, Z. S., and Lim, L. (1994) *Nature* **367,** 40–46
24. Dan, C., Nath, N., Liberto, M., and Minden, A. (2002) *Mol. Cell. Biol.* **22,** 567–577
25. Obermeier, A., Ahmed, S., Manser, E., Yen, S. C., Hall, C., and Lim, L. (1998) *EMBO J.* **17,** 4328–4339
26. Daniels, R. H., Hall, P. S., and Bokoch, G. M. (1998) *EMBO J.* **17,** 754–764
27. Lehmann, J. M., Riethmuller, G., and Johnson, J. P. (1990) *Nucleic Acids Res.* **18,** 1048
28. Bagrodia, S., Taylor, S. J., Creasy, C. L., Chernoff, J., and Cerione, R. A. (1995) *J. Biol. Chem.* **270,** 22731–22737
29. Bokoch, G. M., Wang, Y., Bohl, B. P., Sells, M. A., Quilliam, L. A., and Knaus, U. G. (1996) *J. Biol. Chem.* **271,** 25746–25749
30. Lu, W., Katz, S., Gupta, R., and Mayer, B. J. (1997) *Curr. Biol.* **7,** 85–94
31. Sells, M. A., Knaus, U. G., Bagrodia, S., Ambrose, D. M., Bokoch, G. M., and Chernoff, J. (1997) *Curr. Biol.* **7,** 202–210
32. Nishimura, R., Li, W., Kashishian, A., Mondino, A., Zhou, M., Cooper, J., and Schlessinger, J. (1993) *Mol. Cell. Biol.* **13,** 6889–6896
33. Park, D., and Rhee, S. G. (1992) *Mol. Cell. Biol.* **12,** 5816–5823
34. Meisenhelder, J., and Hunter, T. (1992) *Mol. Cell. Biol.* **12,** 5843–5856
35. Tang, J., Feng, G. S., and Li, W. (1997) *Oncogene* **15,** 1823–1832
36. Galisteo, M. L., Chernoff, J., Su, Y. C., Skolnik, E. Y., and Schlessinger, J. (1996) *J. Biol. Chem.* **271,** 20997–21000
37. Rockow, S., Tang, J., Xiong, W., and Li, W. (1996) *Oncogene* **12,** 2351–2359
38. Oh, W. K., Yoo, J. C., Jo, D., Song, Y. H., Kim, M. G., and Park, D. (1997) *Biochem. Biophys. Res. Commun.* **235,** 794–798
39. Koh, C. G., Manser, E., Zhao, Z. S., Ng, C. P., and Lim, L. (2001) *J. Cell Sci.* **114,** 4239–4251
40. Kim, S., Kim, T., Lee, D., Park, S. H., Kim, H., and Park, D. (2000) *Biochem. Biophys. Res. Commun.* **272,** 721–725
41. Bagrodia, S., Taylor, S. J., Jordon, K. A., Van Aelst, L., and Cerione, R. A. (1998) *J. Biol. Chem.* **273,** 23633–23636
42. Feng, Q., Albeck, J. G., Cerione, R. A., and Yang, W. (2002) *J. Biol. Chem.* **277,** 5644–5650
43. Bagrodia, S., Bailey, D., Lenard, Z., Hart, M., Guan, J. L., Premont, R. T., Taylor, S. J., and Cerione, R. A. (1999) *J. Biol. Chem.* **274,** 22393–22400
44. Turner, C. E., Brown, M. C., Perrotta, J. A., Riedy, M. C., Nikolopoulos, S. N., McDonald, A. R., Bagrodia, S., Thomas, S., and Leventhal, P. S. (1999) *J. Cell Biol.* **145,** 851–863
45. Zhao, Z. S., Manser, E., Loo, T. H., and Lim, L. (2000) *Mol. Cell. Biol.* **20,** 6354–6363
46. Kim, S., Lee, S. H., and Park, D. (2001) *J. Biol. Chem.* **276,** 10581–10584
47. Yoshii, S., Tanaka, M., Otsuki, Y., Wang, D. Y., Guo, R. J., Zhu, Y., Takeda, R., Hanai, H., Kaneko, E., and Sugimura, H. (1999) *Oncogene* **18,** 5680–5690
48. Kim, E. G., Kwon, H. M., Burrow, C. R., and Ballermann, B. J. (1993) *Am. J. Physiol.* **264,** F66–F73
49. Bustelo, X. R. (2000) *Mol. Cell. Biol.* **20,** 1461–1477
50. Fleming, I. N., Elliott, C. M., Collard, J. G., and Exton, J. H. (1997) *J. Biol. Chem.* **272,** 33105–33110
51. Zhao, Z. S., Manser, E., Chen, X. Q., Chong, C., Leung, T., and Lim, L. (1998) *Mol. Cell. Biol.* **18,** 2153–2163
52. Daniels, R. H., Zenke, F. T., and Bokoch, G. M. (1999) *J. Biol. Chem.* **274,** 6047–6050
53. Cowley, S., Paterson, H., Kemp, P., and Marshall, C. J. (1994) *Cell* **77,** 841–852
54. Pang, L., Sawada, T., Decker, S. J., and Saltiel, A. R. (1995) *J. Biol. Chem.* **270,** 13585–13588
55. Hadari, Y. R., Kouhara, H., Lax, I., and Schlessinger, J. (1998) *Mol. Cell. Biol.* **18,** 3966–3973
56. Meakin, S. O., and MacDonald, J. I. (1998) *J. Neurochem.* **71,** 1875–1888
57. Grewal, S. S., York, R. D., and Stork, P. J. (1999) *Curr. Opin. Neurobiol.* **9,** 544–553
58. Robinson, M. J., Stippec, S. A., Goldsmith, E., White, M. A., and Cobb, M. H. (1998) *Curr. Biol.* **8,** 1141–1150

59. Rudel, T., and Bokoch, G. M. (1997) *Science* **276,** 1571–1574
60. Nunn, M. F., and Marsh, J. W. (1996) *J. Virol.* **70,** 6157–6161
61. Renkema, G. H., Manninen, A., Mann, D. A., Harris, M., and Saksela, K. (1999) *Curr. Biol.* **9,** 1407–1410
62. Roig, J., Tuazon, P. T., Zipfel, P. A., Pendergast, A. M., and Traugh, J. A. (2000) *Proc. Natl. Acad. Sci. U. S. A.* **97,** 14346–14351
63. Chong, C., Tan, L., Lim, L., and Manser, E. (2001) *J. Biol. Chem.* **276,** 17347–17353
64. Bokoch, G. M., Reilly, A. M., Daniels, R. H., King, C. C., Olivera, A., Spiegel, S., and Knaus, U. G. (1998) *J. Biol. Chem.* **273,** 8137–8144
65. King, C. C., Gardiner, E. M., Zenke, F. T., Bohl, B. P., Newton, A. C., Hemmings, B. A., and Bokoch, G. M. (2000) *J. Biol. Chem.* **275,** 41201–41209
66. Aghazadeh, B., Zhu, K., Kubiseski, T. J., Liu, G. A., Pawson, T., Zheng, Y., and Rosen, M. K. (1998) *Nat. Struct. Biol.* **5,** 1098–1107
67. Han, J., Luby-Phelps, K., Das, B., Shu, X., Xia, Y., Mosteller, R. D., Krishna, U. M., Falck, J. R., White, M. A., and Broek, D. (1998) *Science* **279,** 558–560
68. Di Cesare, A., Paris, S., Albertinazzi, C., Dariozzi, S., Andersen, J., Mann, M., Longhi, R., and de Curtis, I. (2000) *Nat. Cell Biol.* **2,** 521–530
69. Brown, M. C., Perrotta, J. A., and Turner, C. E. (1998) *Mol. Biol. Cell* **9,** 1803–1816
70. Petit, V., Boyer, B., Lentz, D., Turner, C. E., Thiery, J. P., and Valles, A. M. (2000) *J. Cell Biol.* **148,** 957–970
71. Matafora, V., Paris, S., Dariozzi, S., and de Curtis, I. (2001) *J. Cell Sci.* **114,** 4509–4520